



US ARMY
LABORATORY COMMAND
MATERIALS TECHNOLOGY LABORATORY

AD

AD-A211 680

MTL TR 89-3

A STUDY OF THE HOT WORKABILITY OF Al-8.5 Wt Pct Mg
ALLOYS FOR ARMOR PLATE APPLICATIONS

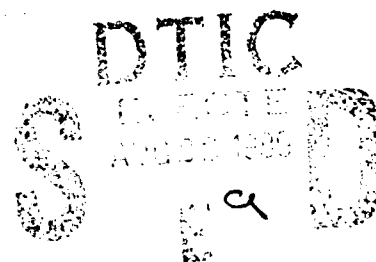
January 1989

JOSEPH R. PICKENS and FRANK H. HEUBAUM
MARTIN MARIETTA CORPORATION
Martin Marietta Laboratories
1450 South Rolling Road
Baltimore, MD 21227

FINAL REPORT

Contract DAAG46-85-C-0034

Approved for public release; distribution unlimited.



Prepared for

U.S. ARMY MATERIALS TECHNOLOGY LABORATORY
Watertown, Massachusetts 02172-0001

89

8

22

017

The findings in this report are not to be construed as an official Department of the Army position, unless so designated by other authorized documents.

Mention of any trade names or manufacturers in this report shall not be construed as advertising nor as an official indorsement or approval of such products or companies by the United States Government

DISPOSITION INSTRUCTIONS

Destroy this report when it is no longer needed
Do not return it to the originator

UNCLASSIFIED

SECURITY CLASSIFICATION OF THIS PAGE (When Data Entered)

REPORT DOCUMENTATION PAGE		READ INSTRUCTIONS BEFORE COMPLETING FORM
1. REPORT NUMBER MTL TR 89-3	2. GOVT ACCESSION NO.	3. RECIPIENT'S CATALOG NUMBER
4. TITLE (and Subtitle) A STUDY OF THE HOT WORKABILITY OF Al-8.5 Wt Pct Mg ALLOYS FOR ARMOR PLATE APPLICATIONS		5. TYPE OF REPORT & PERIOD COVERED Final Report May 1985 - January 1989
7. AUTHOR(s) Joseph R. Pickens and Frank H. Heubaum		6. PERFORMING ORG. REPORT NUMBER MML TR 894(c) ✓
9. PERFORMING ORGANIZATION NAME AND ADDRESS MARTIN MARIETTA CORPORATION Martin Marietta Laboratories, 1450 Rolling Road Baltimore, MD 21227		8. CONTRACT OR GRANT NUMBER(s) DAAG46-85-C-0034
11. CONTROLLING OFFICE NAME AND ADDRESS U.S. Army Materials Technology Laboratory ATTN: SLCMT-PR Watertown, MA 02172-0001		10. PROGRAM ELEMENT, PROJECT, TASK AREA & WORK UNIT NUMBERS
14. MONITORING AGENCY NAME & ADDRESS (if different from Controlling Office)		12. REPORT DATE January 1989
		13. NUMBER OF PAGES 59
		15. SECURITY CLASS. (of this report) Unclassified
		15a. DECLASSIFICATION/DOWNGRADING SCHEDULE
16. DISTRIBUTION STATEMENT (of this Report) Approved for public release; distribution unlimited.		
17. DISTRIBUTION STATEMENT (of the abstract entered in Block 20, if different from Report)		
18. SUPPLEMENTARY NOTES COR - M. WELLS		
19. KEY WORDS (Continue on reverse side if necessary and identify by block number) Aluminum-magnesium alloy Homogenization Rolling (metallurgy) Armor plate Purity effects Hot torsion test Aluminum alloys		
20. ABSTRACT (Continue on reverse side if necessary and identify by block number) (SEE REVERSE SIDE)		

ABSTRACT

Hot-torsion tests were conducted to examine the hot workability of standard and enhanced purity Al-8.5 wt% Mg ingots in both the as-cast and homogenized conditions. The enhanced purity variant showed substantially higher hot ductilities at all homogenization and deformation temperatures investigated with no change in equivalent tensile flow stress. The optimum homogenization practice consists of two stages, namely stage-1 for >5 h at 427°C (800°F) plus >6 h at 482°C (900°F) which provides an equivalent tensile strain-to-failure of approximately 3 as opposed to 1 in the as-cast condition at a strain rate of 0.1 s⁻¹. The optimal strain rate for hot working this Al-8.5 wt% Mg alloy is considerably lower than the nominal 1.2 s⁻¹ typically used in commercial practice for many other Al-Mg alloys. In particular, a strain rate between approximately 0.1 and 0.01 s⁻¹ gives the highest measured strain-to-failure for the alloys containing 0 and 2 ppm sodium. High strain rates and/or higher deformation temperatures promote a brittle quasi-cleavage fracture morphology that reflects the alloy's low ductility under these normal commercial hot-working conditions. A rolling trial using laboratory-scale ingots was successfully conducted with minimal edge cracking using the parameters determined from the hot-torsion tests.

[illegible]

TABLE OF CONTENTS

	<u>Page</u>
ABSTRACT	i
LIST OF FIGURES	ii
LIST OF TABLES	iv
I. INTRODUCTION	1
II. MATERIALS AND EXPERIMENTAL PROCEDURES	5
A. PHASE I	5
B. PHASE II	9
C. PHASE III	10
D. ROLLING TRIAL	14
III. RESULTS	19
A. PHASE I	19
B. PHASE II	23
C. PHASE III	35
D. ROLLING STUDY	41
IV. DISCUSSION	45
V. SUMMARY	52
VI. CONCLUSIONS	54
VII. RECOMMENDATIONS	55
VIII. REFERENCES	56
IX. ACKNOWLEDGEMENTS	59

LIST OF FIGURES

<u>Figure</u>		<u>Page</u>
1	Hot-mill recovery of Al-Mg alloy vs total sodium content. Courtesy H. Shillinglaw, from memo to J. Pickens 1979 [The exact Na levels are not provided for proprietary reasons.]	3
2	Schematic of hot-torsion specimen.	7
3	Configuration and dimensions for rolling ingots	16
4	(a) Equivalent tensile flow stress and b) strain-to-failure of as-cast specimens deformed by hot torsion at various temperatures.	20
5	Optical micrographs of the as-cast structure of commercial- and enhanced-purity Al-8.5wt% Mg alloys.	21
6	Effect of homogenization temperature on a) equivalent tensile flow stress and b) equivalent tensile strain-to-failure for torsion specimens deformed at 315°C (600°F).	22
7	(a) Flow stress and (b) strain-to-failure variation with homogenization temperature for hot torsion tests conducted at 427°C (800°F). The results for 2 ingots of each purity level are plotted.	24
8	Alloy purity and strain rate effects on equivalent tensile strain-to-failure for specimens homogenized at different temperatures. Homogenization temperatures are stage-2 for 8 h each and follow a stage-1 practice of 427°C (800°F) for 16 h.	25
9	Homogenization time has little influence on equivalent tensile flow stress.	27
10	Variation of strain-to-failure with homogenization time showing an increase up to ~6 h.	28
11	Optical micrographs of enhanced-purity alloy showing interdendritic MnAl ₆ precipitation and coarsening during stage-2 homogenization at 482°C (900°F) for various lengths of time: (a) 0 h, (b) 2 h, and (c) 12 h.	29
12	Equivalent tensile flow stress decreases linearly with deformation temperature at strain rates of 0.1 s ⁻¹ and 1.2 s ⁻¹ .	30
13	Equivalent tensile strain-to-failure peaks at deformation temperatures between 425 and 460°C (800 and 850°F).	32

LIST OF FIGURES (cont.)

<u>Figure</u>		<u>Page</u>
14	Scanning electron fractographs of hot-torsion specimens deformed at 426°C showing (a) ductile shear failure at a strain rate of 0.1 s^{-1} and (b) region of quasi-cleavage at 1.2 s^{-1} . Increasing deformation temperature results in similar quasi-cleavage failure.	33
15	Deformed hot torsion specimens of (a) enhanced-purity and (b) enhanced-purity with 0.05 wt% Ti, showing that the rumpling of the surface during deformation decreases with the addition of Ti to the ingot.	34
16	Equivalent tensile flow stress a) is unaffected by Na content and equivalent tensile strain-to-failure b) decreases above 10 ppm Na in hot torsion tests of Al-8.5% Mg alloys tested at 427°C and a shear strain rate of 0.1 s^{-1} .	38
17	Flow stress increases linearly with strain rate as measured using both hot torsion and hot compression testing. Strain-to-failure increases substantially with decreasing strain rate, changing from a cleavage to a ductile fracture mode. ($T_{\text{DEF}} = 427^\circ\text{C}$ (800°F))	39
18	Equivalent tensile flow stress and strain-to-failure of Al-8.5 wt% Mg alloy with 2 ppm sodium tested by hot torsion at 427°C (800°F) and varying strain rates.	40
19	Photograph of Al-8.5% Mg plate that was rolled at the optimum conditions determined from the hot-torsion tests (left) and plate rolled at a strain rate of 1 s^{-1} , which cracked severely.	42
20	Scanning electron micrograph showing a quasi-cleavage fracture mode in rolling ingot #2 which was rolled at a strain rate of $\sim 1 \text{ s}^{-1}$.	44
21	Hardness increases with stage-1 homogenization time as increased Mg goes into solid solution and submicron MnAl_6 precipitates from supersaturated solid solution.	47
22	Optical polarized light micrograph of a longitudinal section of a hot-torsion specimen showing recrystallized grains near the outer diameter and nearly undistorted grains at the neutral central axis.	49

LIST OF TABLES

<u>No.</u>		<u>Page</u>
I	Chemical Analysis of Master Alloy Charge (wt%)	5
II	Ingot Compositional Analysis in Weight Percent [Inductively Coupled Plasma (ICP) Technique]	8
III	Chemical Analysis (in wt%) of Al-8.5% Mg Ingots Showing Variation Between Different Measurement Techniques at Various Laboratories	12
IV	Chemical Analysis (wt%) of Al-Mg Alloys with Sodium Additions	13
V	Chemical Analysis of Rolling Ingots	14
VI	Hot-Rolling Schedule	17
VII	Cold-Rolling Schedule	18
VIII	Hot-Torsion Data for Al-8.5% Mg Alloys with Varying Na Content	36
IX	Strain-Rate Effects on Hot Torsion Study of Al-8.5% Mg. Tested at 427°C (800°F)	37

1. INTRODUCTION

Aluminum magnesium alloys are technologically useful for their medium-to-high strength, low density, good corrosion resistance, and weldability, which varies from acceptable to excellent. The strength of this alloy subsystem results primarily from Mg solid-solution strengthening and a very strong cold-working response. Alloy strength generally increases with increasing Mg content, but the amount of Mg that can be practically alloyed is limited by susceptibility to stress-corrosion cracking (SCC) and by reduced hot workability. Indeed, the most commonly used Al-Mg alloys rarely have above about 5 wt% Mg because of these problems.

Al-Mg alloys with 4-5 wt% Mg are extensively used for armor plate applications, but designers would like to have Al-Mg alloys available at higher strength levels. Development of Al-8.5 wt% Mg alloys has shown the promise of increased strength, which may provide the potential for improved ballistic performance, but poor hot workability has been a problem limiting alloy introduction. Specifically, aluminum alloys containing 8.5 wt% Mg have a tendency for severe edge cracking when rolled into plate and sheet.

Edge cracking in Al-Mg alloys has been shown to correlate with sodium impurities,⁽¹⁻⁴⁾ which are expensive to reduce below certain levels. In addition, Al-Mg alloys are embrittled at hot working temperatures by sodium levels that have no adverse effect on other alloys.

Talbot and Ransley^(1,2) have proposed an explanation for the embrittling effect of sodium. They suggest that free sodium, i.e., not chemically bound, moves freely in aluminum alloys and is absorbed on internal crack surfaces or grain boundaries, which leads to embrittlement. Silicon, an impurity in virtually all commercial aluminum as well as Al-Mg alloys, immobilizes the sodium by forming a Na-Al-Si complex, thereby decreasing its embrittling effect. However, in aluminum alloys containing more than about 2 wt% Mg, Mg_2Si precipitation occurs preferentially, thereby leaving the Na free to cause embrittlement.

Significant scrap losses can occur from sodium impurity in Al-Mg alloys. For example, mill recovery of Al-4.4 wt% Mg alloy 5182 is quite high, ~ 80%, at low sodium levels, but decreases sharply and drastically to less than 20% at higher levels (see Fig. 1). Such mill recovery data are acquired from production problems, painfully and expensively, but are obviously not available as a new alloy is introduced. Furthermore, commercial-scale experiments that assess material loss from edge cracking, or address other hot working issues, are not practical because of the expense of casting and scrapping 10,000- to 20,000-lb ingots containing different sodium levels. Consequently, laboratory-scale hot-working simulators have been developed to efficiently optimize hot working practices. The hot-torsion machine⁽⁵⁻⁷⁾ is perhaps the most advantageous such simulator because it provides information on the material's resistance to deformation (flow stress) and hot ductility (strain-to-failure); the latter is related to edge cracking resistance.

The hot-torsion machine has been utilized to optimize homogenization practices for several commercial Al-Mg alloys,^(8,9) as well as to identify advantageous hot working regimes, i.e., those with relatively low flow stress and high strain-to-failure. In addition, it has been used to compare the hot workability of Al-Mg alloys cast by different techniques. For example, Pickens et al.⁽⁸⁾ compared the workability of Al-4.4 wt% Mg alloy 5182 cast conventionally, i.e., by the direct chill (DC) casting process, and by electromagnetic casting (EMC). The 5182 EMC displayed greater hot ductility than the 5182 DC which was attributed to the former's finer cast structure. In addition, when the homogenization practices for each were optimized, the 5182 EMC responded more quickly to homogenization, once again because of its finer structure.

Precht and Pickens⁽⁹⁾ also used the hot torsion machine to optimize the hot-working practice of Al-2.5 wt% Mg alloy 5052. Homogenization temperature and time, as well as deformation temperature and strain rate, were optimized using this lab-scale simulator. The hot-working parameters identified by hot torsion reduced edge cracking in a plant trial.⁽¹⁰⁾

In the present investigation, the hot workability of Al-8.5 wt% Mg alloys is studied by hot torsion testing to develop homogenization schedules,

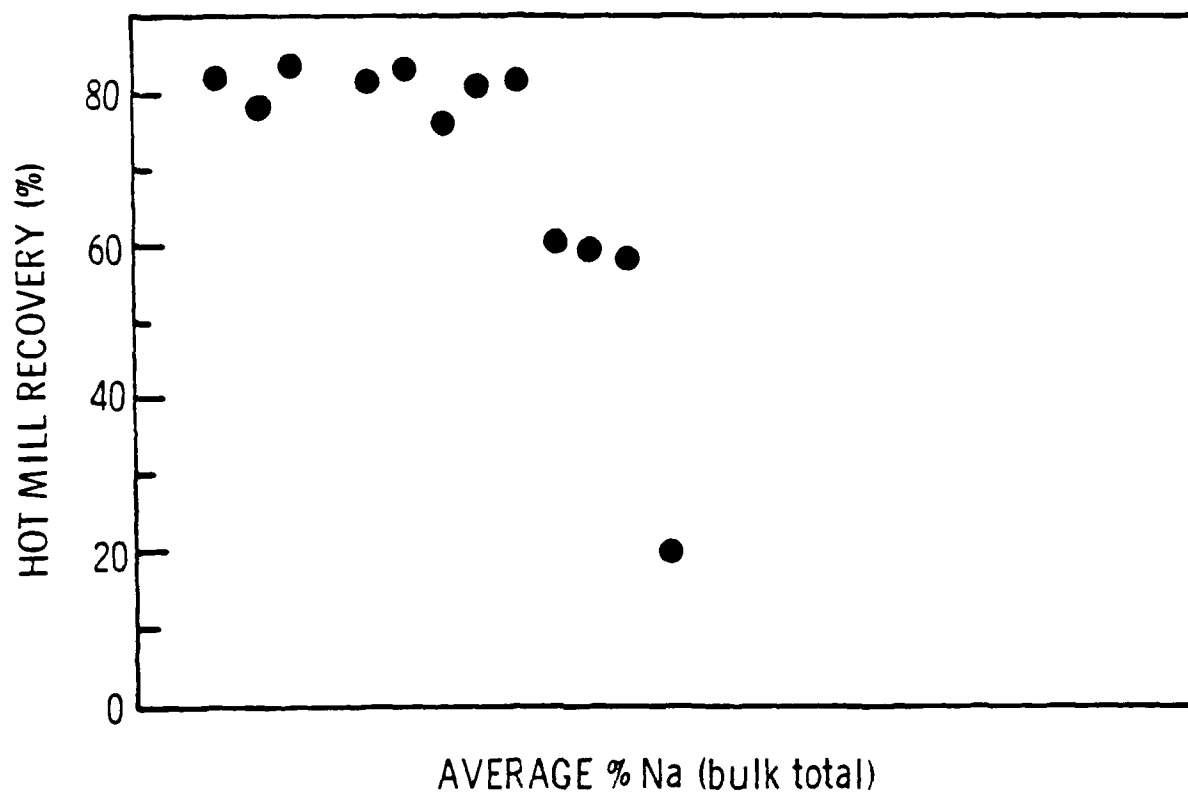


Fig. 1 Hot-mill recovery of Al-Mg alloy vs total sodium content.
Courtesy H. Shillinglaw, from memo to J. Pickens 1979
[The exact Na levels are not provided for proprietary reasons.]

Identify advantageous hot-working temperatures and strain rates, and assess the effect of sodium impurity on edge cracking. Because edge cracking of Al-8.5 wt% Mg alloys is a major factor that currently limits their acceptance, it is hoped that insights obtained from this study might help to make such alloys commercially viable.

II. MATERIALS AND EXPERIMENTAL PROCEDURES

During this program, much effort was expended in preparing suitable model alloys for evaluation. Accurate measurement of Na content was extremely difficult, yet important before performing the major thrust of the program--hot-torsion testing. Consequently, the following section on materials and experimental procedures is necessarily detailed.

A. PHASE I

The Al-8.5% Mg* alloys used in this study were prepared using induction melting furnaces manufactured by Ajax Magnethermic Corporation (1250 V, 2400 KVA, 1920 A, 100 kW, 3000 Hz) and clay-bonded graphite crucibles. Cylindrical ingots nominally 16 cm (6.3 in.) in diameter and 35 cm (14 in.) in height and weighing approximately 20 kg (44 lb) were cast in a water-cooled bronze mold. The charge material used for the castings was 99.99% pure aluminum pig produced by Alcoa and master alloys from the KBI Division of Cabot Corporation. The compositions are given in Table I.

Table I
Chemical Analysis of Master Alloy Charge (wt%)

	<u>Mg</u>	<u>Mn</u>	<u>Cr</u>	<u>Si</u>	<u>Fe</u>	<u>Cu</u>	<u>Zn</u>
Al	0.003	0.001	0.001	<0.01	0.007	-	-
Al-Mg	24.7	0.003	0.003	0.015	0.084	-	-
Al-Cr	<0.01	0.004	9.47	0.059	0.16	-	-
Al-Mn	<0.01	23.5	0.005	0.047	0.050	-	-
Al-Si	<0.002	0.004	0.002	50.5	0.12	0.002	0.006
Al-Cu	<0.002	0.004	0.002	0.057	0.20	20.9	0.067
Fe	0.18	0.03	0.08	0.03	bal	0.27	0.23

*Unless stated otherwise, this notation denotes weight percent.

A 12 cm (5 in.) insulating ceramic fiber extension on top of the mold was devised and utilized as a hot-top to minimize the extent of the pipe defect during ingot solidification. Standard chlorine-pellet fluxing was used to reduce gas porosity due to dissolved hydrogen and also to scavenge sodium impurities. However, chlorine readily combines with the magnesium to form MgCl_2 and $\text{MgCl}_2 \cdot \text{MgO}$, which float to the surface as slag and dross. Thus, for the specific melt size used (23 kg; 50 lb) and fluxing technique, it was determined that a total addition of 9.2% Mg was required to yield the desired 8.5% Mg. The ingots were poured at a nominal temperature of 670°C (1240°F) which is a relatively low melt superheat. Low superheat, along with the water cooling of the mold, refines dendrite and cell size, thereby leading to increased homogeneity.

The effect of alloy purity on hot workability was examined by casting commercial- and enhanced-purity variants of the alloy containing nominally Al-8.5Mg-0.5Mn-0.1Cr-0.4Fe-0.25Si-0.1Cu-0.2Zn and Al-8.5Mg-0.5Mn-0.1Cr-0.05Fe-0.05Si-0.01Cu-0.01Zn (wt%), respectively, with less than 1 ppm Na by weight. The measured chemical compositions of the ingots are given in Table II.

Hot torsion specimens of dimensions shown in Fig. 2 were machined from as-cast and homogenized blanks at equiradial locations 1.5 cm (0.75 in.) beneath the ingot surface. This location was chosen such that all sample blanks were within the equiaxed grain region of the casting, away from the columnar grains growing inward from the surface. In addition, inverse segregation results in a surface region enriched in impurities and magnesium. For example, a chemical analysis of the first standard purity ingot at a location 2 mm beneath the surface showed Al-9.59Mg-0.51Mn-0.10Cr-0.14Si-0.46Fe-0.14Cu-0.17Zn. The homogenization treatments investigated consisted of solutionizing at 427°C (800°F) for 16 h followed by an additional 8 h at one of four temperatures between 471 and 504°C (880, 900, 920, and 940°F). The initial 427°C treatment was required to dissolve the nonequilibrium eutectic phases into solid solution, as will be discussed. Selected samples were hot isostatically pressed (HIPed) to determine whether casting porosity was affecting strain-to-failure.

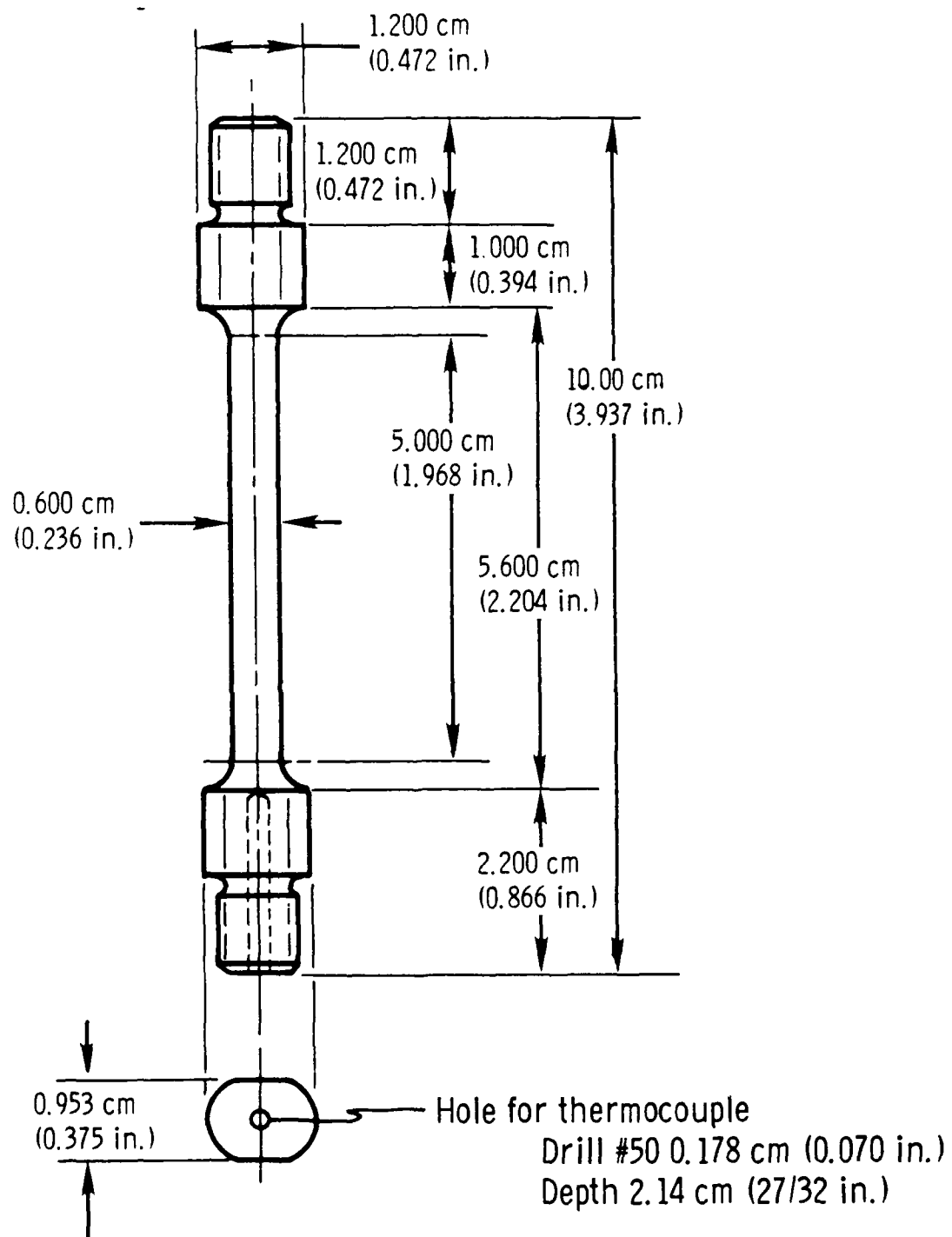


Fig. 2 Schematic of hot torsion specimen.

Table II
Ingot Compositional Analysis in Weight Percent
 (Inductively Coupled Plasma (ICP) Technique)

	<u>Mg</u>	<u>Mn</u>	<u>Cr</u>	<u>Si</u>	<u>Fe</u>	<u>Cu</u>	<u>Zn</u>	<u>Na</u> *
<u>Standard Purity</u>								
1	8.66	0.50	0.10	0.10	0.38	0.11	0.15	--
2	8.63	0.48	0.10	0.22	0.39	0.12	0.21	0
3	8.20	0.51	0.11	0.14	0.31	0.09	0.11	0
<u>Enhanced Purity</u>								
1	8.70	0.48	0.10	0.08	0.049	>0.002	0.002	--
2	8.47	0.49	0.10	0.044	0.086	0.002	0.002	0
3	8.59	0.53	0.094	0.011	0.044	0.002	0.002	0
4	8.78	0.53	0.10	0.037	0.053	0.003	0.003	0

* Sodium analysis below 1 ppm detection limit using optical emission technique at both Reynolds Metals Co. and Commonwealth Aluminum. Scatter and insufficient precision occurred when using ICP.

Hot-torsion tests were initially conducted at an equivalent tensile strain rate of 1.2 s^{-1} at a deformation temperature of 471°C (880°F) to examine the effects of alloy purity and homogenization practice on hot workability. However, under these testing conditions, the extremely low ductility (strain-to-failure <0.05) precluded an accurate assessment of these variables. As-cast specimens were then deformed at 260 to 427°C (500, 600, 700, and 800°F) to determine a suitable deformation temperature for the homogenization study. Later it was learned that a lower strain rate, namely 0.1 s^{-1} , was a more appropriate testing parameter and subsequent tests were performed at this strain rate and a deformation temperature of 427°C (800°F).

The equivalent tensile flow stress (σ_0) for each hot torsion test was calculated from the maximum applied torque (M) achieved during deformation

using both the Von Mises criterion and the simplified Fields Backofen equation (11):

$$\sigma_0 = 3\sqrt{3} M/2\pi r^3$$

where r is the radius of the specimen gauge section. The equivalent tensile true strain-to-failure (ϵ_f) was calculated from the true surface shear strain at failure (γ_f) and the Von Mises criterion:

$$\epsilon_f = \frac{\gamma_f}{\sqrt{3}}$$

where γ_f is given by:

$$\gamma_f = \frac{r\theta}{L}$$

where L is the gauge length and θ is the angular displacement at failure.

The hot torsion tests were conducted with unconstrained axial motion to prevent axial stresses from developing during the tests. The axial displacements were measured continuously during each test with a linear variable differential transducer (LVDT). The specimen elongations never exceeded 300 μm before failure and therefore little error was associated with this parameter.

B. PHASE II

The enhanced-purity composition of Phase I was used to optimize the homogenization time and deformation temperature of the alloy. A two-stage homogenization schedule was found to be necessary since metallographic examination showed the presence of non-equilibrium eutectic β phase (Mg_2Al_3) which would cause liquation above 450°C (842°F). Sample coupons were homogenized at a series of times between 0 and 16 h at 427°C (800°F) and metallographically examined to determine the length of time required to bring

the β phase into solution for stage-1 homogenization. Stage-2 homogenization of hot-torsion specimens was performed between 0 and 12 hours in two-hour increments at 482°C (900°F), which was determined to be the optimum temperature in Phase I. Using the hot torsion results, including flow stress and strain-to-failure, the optimum homogenization schedule was determined.

The preferred working temperature for the alloy was determined by conducting hot torsion tests on both as-cast and 8-hour stage-2 homogenized specimens. Deformation temperature was varied between 315°C and 504°C (600, 700, 750, 800, 850, 900, and 940°F) to determine the temperature giving the best combination of high ϵ_f and low σ_0 . Tests were conducted at strain rates of 1.2 and 0.1 s⁻¹.

C. PHASE III

The objective of the Phase III research was to evaluate the influence of sodium impurity at levels ranging from 0 to 6 ppm, and of strain rate on the hot workability of Al-8.5% Mg alloys. Results of Phase I chemical analyses at Martin Marietta Laboratories (the Labs) of the initial ingots, using both ICP and atomic absorption (AA) techniques, revealed apparently very high levels of sodium (> 100 ppm). After recasting with improved fluxing and vacuum melting procedures, internal chemical analyses at the Labs still revealed considerable scatter in sodium levels. Consequently, 6.3 cm (2.5 in.) diameter disc specimens were machined from these ingots and sent to Commonwealth Aluminum (CA) in Lewisport, KY, for analysis using optical emission - spark discharge spectroscopy. No sodium was detected, with a claimed resolution of better than 0.1 ppm. The subsequent work for Phases I and II was performed using these ingots.

In Phase III assessment of the effect of sodium on workability, small amounts of sodium dichromate ($\text{Na}_2\text{Cr}_2\text{O}_7 \cdot 2\text{H}_2\text{O}$) were added to the alloy in an attempt to adjust the sodium level to 0-6 ppm. This compound was selected because chromium is used as an alloying element; the compound contains no other elements that would be expected to influence workability. The water of

hydration, which is known to evolve at 100°C, was removed by preliminary baking to eliminate the risk of explosion while adding the compound to the melt. The compound $\text{Na}_2\text{Cr}_2\text{O}_7$ is reported to decompose at 400°C; well below the temperature of the molten alloy when added (720°C).

Standards for sodium in an Al-10% Mg matrix were purchased from Alcoa to calibrate and verify the analytical equipment. Chemical analyses were then performed at the Labs, Commonwealth Aluminum (CA), and (when inconsistencies again arose) at National Southwire Aluminum (NSA), as shown in Table III. Both CA and NSA reported very high Mg values. However, these two companies do not work with Mg levels in aluminum alloys above 5 and 7%, respectively, and lack the appropriate standards for the quantification of Mg above these levels.

A rolling trial was then conducted at the Reynolds Metals Company Laboratory, in Richmond, VA, and samples of the ingots were chemically analyzed using spark discharge spectroscopy. Sodium standards 1 and 2 showed 20 and 40+ ppm Na, respectively, whereas ingots 3, 4, and 5 all showed <1 ppm Na, with 8.5, 8.2, and 8.8% Mg, respectively. Other ingots with the sodium dichromate additions also showed no detectable sodium (<1 ppm).

Subsequent discussions with Reynolds Laboratory personnel concerning their experience with sodium-modified casting alloys containing silicon suggested an alternative procedure for adding the Na to the Al-Mg alloy. Sodium is added to Al-Si alloys to modify the morphology of the eutectic $(\text{Al-Si})_x$ clusters. Pure (dry) sodium wrapped in aluminum foil is vigorously stirred into the melt using a graphite rod as a stir bar. With this method, the level of Na added is typically several times greater than the intended level in the ingot due to large melt losses.

Two enhanced-purity heats of 25 kg (55 lb) were made. For each heat, sodium was added incrementally to the crucible following each pouring of the melt into thick-walled mild-steel molds having an internal diameter of 10 cm (4 in.) and a height of 25 cm (10 in.). In this way, the overall composition of each casting would be maintained constant, except for varied sodium levels.

Table III

Chemical Analysis (in wt%) of Al-8.5% Mg Ingots

Showing Variation Between Different Measurement Techniques
at Various Laboratories

<u>Ingot</u>	<u>Vendor</u>	<u>Mg</u>	<u>Mn</u>	<u>Cr</u>	<u>Si</u>	<u>Fe</u>	<u>Cu</u>	<u>Zn</u>	<u>Na (ppm)</u>
3	Labs	8.59	0.53	0.094	0.011	0.044	0.002	0.002	< 10*
	CA	11.8	0.36	0.09	0.04	0.05	0.001	0.004	0
	NSA	9.3	0.48	0.08	0.03	0.05	0.002	0.005	3
	Reynolds	8.2	-	-	-	-	-	-	< 1
4	Labs	8.78	0.53	0.10	0.037	0.053	0.003	0.003	< 10*
	CA	10.6	0.40	0.09	0.05	0.06	0.004	0.002	0
	NSA	9.58	0.51	0.09	0.05	0.06	0.005	0.008	2
	Reynolds	8.5	-	-	-	-	-	-	< 1
5	Labs	8.28	0.50	0.11	0.02	0.07	0.01	0.003	< 10*
	CA	13.1	0	0.11	0	0	0.004	0	0
	Reynolds	8.8	-	-	-	-	-	-	< 1
Standard 1	Alcoa	-	-	-	-	-	-	-	2(0)**
	Labs	-	-	-	-	-	-	-	24, 28
	CA	-	-	-	-	-	-	-	30
	Reynolds	-	-	-	-	-	-	-	20+
Standard 2	Alcoa	-	-	-	-	-	-	-	4(8)**
	Labs	-	-	-	-	-	-	-	54, 51
	CA	-	-	-	-	-	-	-	90
	Reynolds	-	-	-	-	-	-	-	40+

* Operator later put resolution limit at 10 ppm

** Second digit not certified by Alcoa, 20 and 48 ppm

The first melt (A) received sequential additions of 54, 23, and 52 mg of sodium; the second (B) received 98, 49, 50, 50, and 50 mg. The chemical analyses are given in Table IV.

Table IV
Chemical Analysis (wt%) of Al-Mg Alloys with Sodium Additions

	<u>Mg</u>	<u>Mn</u>	<u>Cr</u>	<u>Si</u>	<u>Fe</u>	<u>Ti</u>	<u>Na (ppm)</u>
<u>Melt A</u>							
1A	9.06	0.51	0.09	0.03	0.08	0.03	< 1
2A	8.98	0.53	0.09	0.05	0.08	0.03	1
3A	9.09	0.51	0.09	0.05	0.08	0.03	2
<u>Melt B</u>							
1B	9.62	0.49	0.09	0.04	0.06	0.03	2
2B	9.41	0.49	0.09	0.04	0.06	0.03	5
3B	9.42	0.50	0.08	0.04	0.06	0.04	5
4B	9.61	0.49	0.09	0.04	0.06	0.03	8
5B	9.66	0.48	0.08	0.04	0.07	0.03	20

Although the planned sodium levels were 0-6 ppm, losses and possible variations throughout each ingot caused some duplication and higher Na levels were obtained. The magnesium levels appear erroneously high, since only 9.2% was added to each melt and losses are known to occur during fluxing. A problem with the standard used in the Mg analysis is the likely cause of this discrepancy.

A preliminary assessment of the effect of strain rate on flow stress and equivalent tensile strain-to-failure was made using hot torsion and hot

compression testing at 427°C (800°F) with ingot 3 of the enhanced purity alloy given in Table III. This ingot was chosen because its sodium content (3 ppm), considered the most accurate at the time of the study, might be the level where the Na begins to adversely affect workability in lower Mg-containing aluminum alloys, as shown in Fig. 1. Selected specimens (0.6 cm dia. x 0.75 cm) were deformed in hot compression to compare flow stress values obtained under different stress states. The Von Mises criterion was used in comparing the data. This ingot was later verified to contain <1 ppm Na. The effect of strain rate on hot workability was again performed with an ingot containing an actual sodium content of 2 ppm, namely ingot 3A.

D. ROLLING TRIAL

Four rectangular ingots (20 kg; ~45 lb), with nominal dimensions 19 x 10 x 43 cm (7.5 x 4 x 17 in.), of the enhanced-purity composition were cast in a steel book mold. In two of the ingots, titanium was present as an additional grain refiner. The chemical analysis of these ingots is given in Table V.

Table V
Chemical Analysis of Rolling Ingots

<u>#</u>	<u>Al</u>	<u>Mg</u>	<u>Mn</u>	<u>Cr</u>	<u>Si</u>	<u>Fe</u>	<u>Ti</u>	<u>Na</u>
1	Bal	8.45	0.43	0.11	0.01	0.04	--	ND*
2	Bal	9.21	0.56	0.11	0.02	0.08	--	ND
3	Bal	8.56	0.56	0.10	0.02	0.07	0.05	ND
4	Bal	9.19	0.53	0.09	0.02	0.06	0.08	ND

* ND - none detected (< 1 ppm)

The ingots were homogenized using the two-step treatment of 427°C (800°F) for 5 h plus 6 h at 482°C (900°F) that was found to be optimal. The heat-up time of 6 h to bring the ingots to 427°C (800°F) and 2 h to 482°C (900°F) is an additional time not expected to greatly influence workability, as demonstrated in Phase II of the program. Following homogenization, the ingots were scalped to a thickness of 8 cm (3 1/8 in.) which was the maximum roll separation available on the Reynolds hot rolling mill where subsequent rolling was to take place. Discussions with Reynolds Laboratory personnel suggested that scalping in excess of 1.2 to 2.5 cm (0.5 to 1 in.) off each side is typical, even in continuous-cast material of high-strength aluminum alloys. A mild 8°-V taper was milled along the side edges and a partial 45° along the leading and tail edges of the ingots, as illustrated in Fig. 3. This type of chamfering system has been previously documented within the aluminum industry to reduce the tendency of some alloys to edge crack and alligator during rolling. A small 2-mm-diameter hole was drilled in a side of each ingot so that a thermocouple to monitor the temperature could be attached.

The ingots were preheated to nominally 470°C (875°F), at which temperature hot rolling was started. The temperature is on the high side of the temperature range for maximum hot ductility, as determined from the hot torsion tests, but was high to allow for cooling as heat is extracted into the rolls. The rolling mill used was a four-high mill, where the diameter of the working rolls was 20.3 cm (8 in.) and the back-up rolls ~ 61 cm (24 in.). The reduction per pass was 3 mm (1/8 in.) or between 4 and 12% reduction depending on thickness. The hot-rolling schedule is given in Table VI. When the plates had been hot rolled to about 2.5 cm (1 in.), they were annealed at 470°C (875°F) for 1/2 hour, cooled to room temperature, and given several cold-rolling passes as required for strengthening 5xxx series alloys. The reduction used was 1.3 mm (0.05 in.) per pass or 4 to 6% reduction. The cold-rolling schedule is given in Table VII.

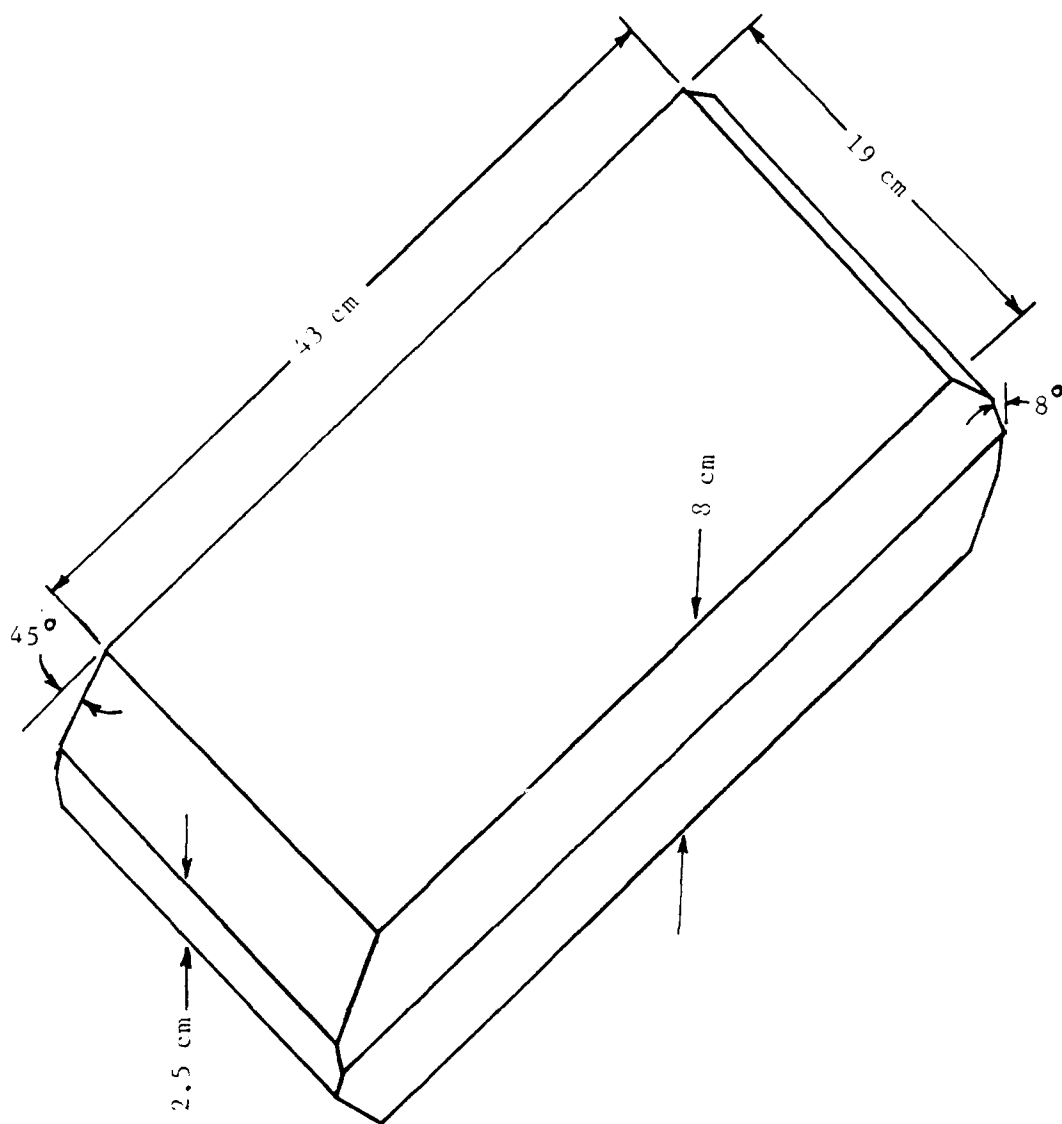


Fig. 3 Configuration and dimensions for rolling ingots

Table VI
Hot-Rolling Schedule

Ingot (#)	Temp. _i *	Temp. _f *	Passes (#)	Thickness		Reduction (%)
	°C (°F)	°C (°F)		cm	(in.)	
1	470 (880)	400 (750)	2	7.3	(2 7/8)	8
	455 (850)	375 (710)	2	6.7	(2 5/8)	16
	472 (880)	---	6	4.8	(1 7/8)	40
	465 (870)	---	3	4.8	(1 1/2)	52
	460 (860)	---	3	2.9	(1 1/8)	64
2	465 (870)	407 (765)	2	7.3	(2 7/8)	8
	470 (875)	405 (760)	2	6.7	(2 5/8)	16
	465 (870)	---	4	5.4	(2 1/8)	32
	465 (870)	---	1			
3	475 (885)	400 (750)	2	7.3	(2 7/8)	8
	460 (860)	388 (730)	2	6.7	(2 5/8)	16
	457 (855)	382 (720)	2	6.0	(2 3/8)	24
	460 (860)	---	4	4.8	(1 7/8)	40
	460 (860)	360 (680)	3	3.8	(1 1/2)	52
	475 (882)	---	2	3.2	(1 1/4)	60
			2	2.5	(1)	68
4	470 (880)	407 (765)	2	7.3	(2 7/8)	8
	465 (870)	400 (750)	2	6.7	(2 5/8)	16
	465 (870)	355 (670)	4	5.4	(2 1/8)	32
	465 (870)	---	3	3.8	(1 1/2)	52
	460 (860)	---	3	2.9	(1 1/8)	64

* i = initial; f = final

Table VII
Cold-Rolling Schedule

Ingot (#)	Initial Thickness cm (in.)	Final Thickness cm (in.)	Passes (#)	Cold Reduction (%)
1	3.18 (1.25)	2.19 (0.86)	6	31
2	Cracked during hot rolling			--
3	2.45 (0.97)	1.92 (0.75)	5	22
4	3.18 (1.25)	2.32 (0.91)	5	27

III. RESULTS

A. PHASE I

As-cast specimens of both enhanced- and standard-purity Al-8.5% Mg alloys underwent hot-torsion testing at various deformation temperatures between 260 and 471°C (500-880°F) at a strain rate of 1.2 s^{-1} to determine a suitable deformation temperature at which to assess the homogenization conditions. Equivalent tensile flow stress decreases monotonically with increasing deformation temperature (Fig. 4) and there is a maximum in equivalent tensile strain-to-failure near 315°C (~600°F). Ductility is clearly higher in the enhanced-purity alloy but flow stress is not significantly affected by alloy purity. The microstructure of both the commercial- and enhanced-purity alloys in the as-cast condition (Fig. 5) consists of:

- | | |
|---|--|
| $\text{S}(\text{Mg}_2\text{Al}_3)$ | - Large rounded or irregular particles primarily on boundaries with smaller particles within the matrix; light white |
| MnAl_6 or $(\text{Mn},\text{Fe})\text{Al}_6$ | - Large blocky/angular particles formed as solid or hollow parallelograms; light grey |
| CrAl_7 | - Needles or elongated polygons; light grey |
| FeAl_3 | - Needle-shaped particles or clusters; grey |
| Mg_2Si | - Script eutectic structure; dark gray or black |

As seen in the optical micrographs in Fig. 5, the enhanced-purity alloy contains a lower volume fraction of constituent particles.

The variations in flow stress and strain-to-failure with homogenization temperature are shown in Fig. 6 for specimens deformed at 315°C (600°F). Only small changes are apparent in these parameters over the range investigated. To evaluate the role of microporosity on the ductility, selected specimens were hot isostatically pressed (HIPed) at 315°C (600°F) and 207 MPa (30 ksi). The HIPed specimens showed an increase in strain-to-failure over

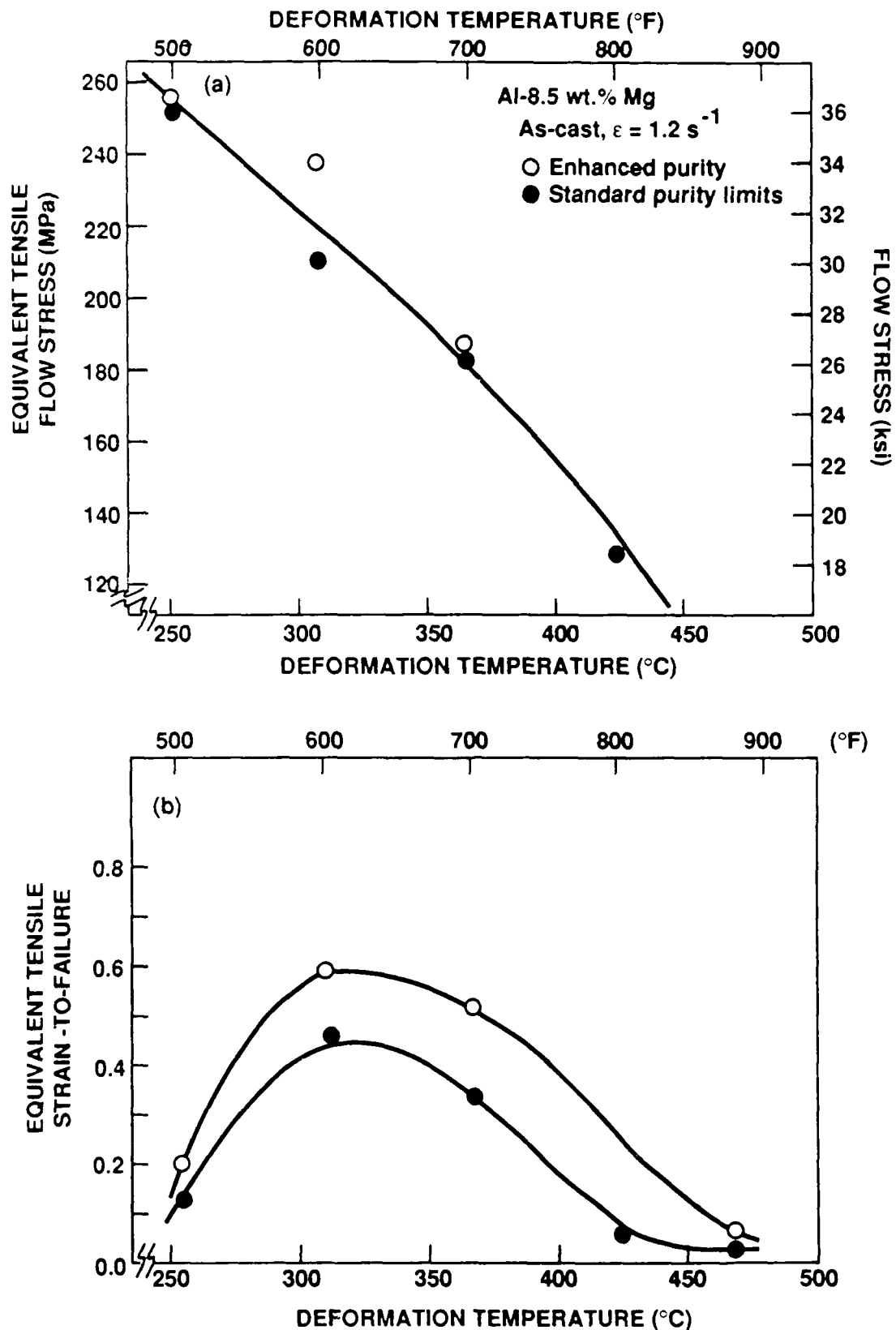
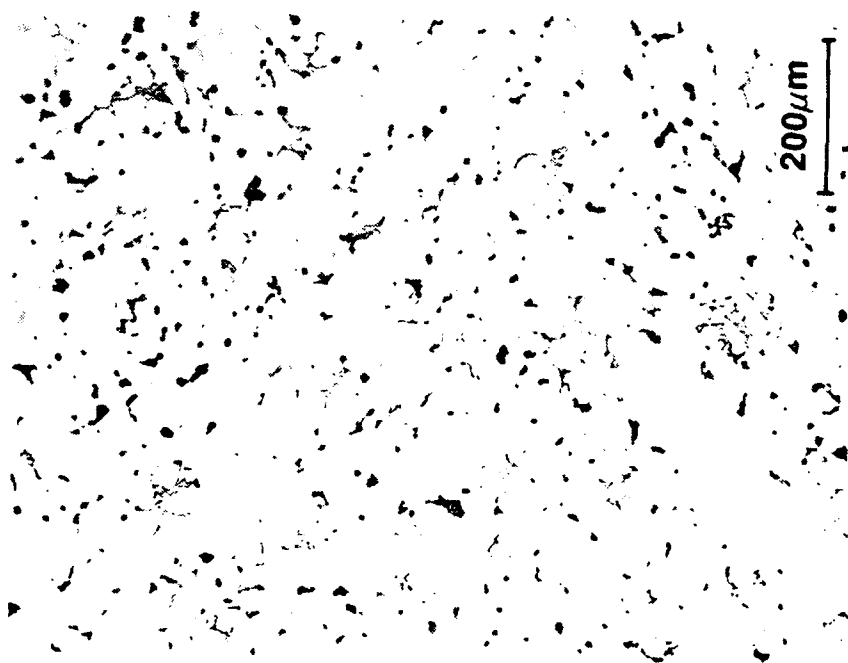


Fig. 4 a) Equivalent tensile flow stress and b) strain-to-failure of as-cast specimens deformed by hot torsion at various temperatures.

AS-CAST MICROSTRUCTURE

COMMERCIAL PURITY



ENHANCED PURITY

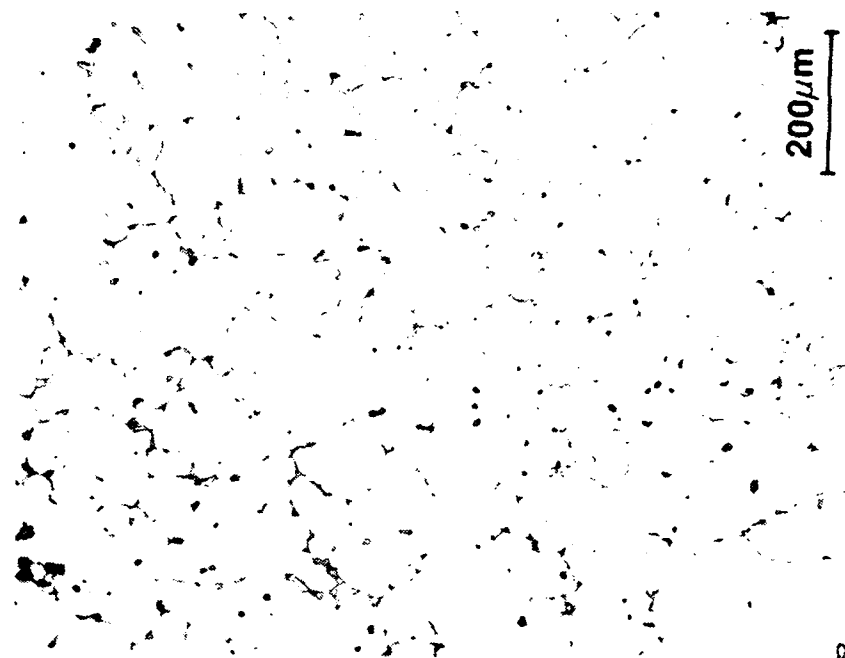


Fig. 5 Optical micrographs of the as-cast structure of commercial- and enhanced-purity Al-8.5wt% Mg alloys.

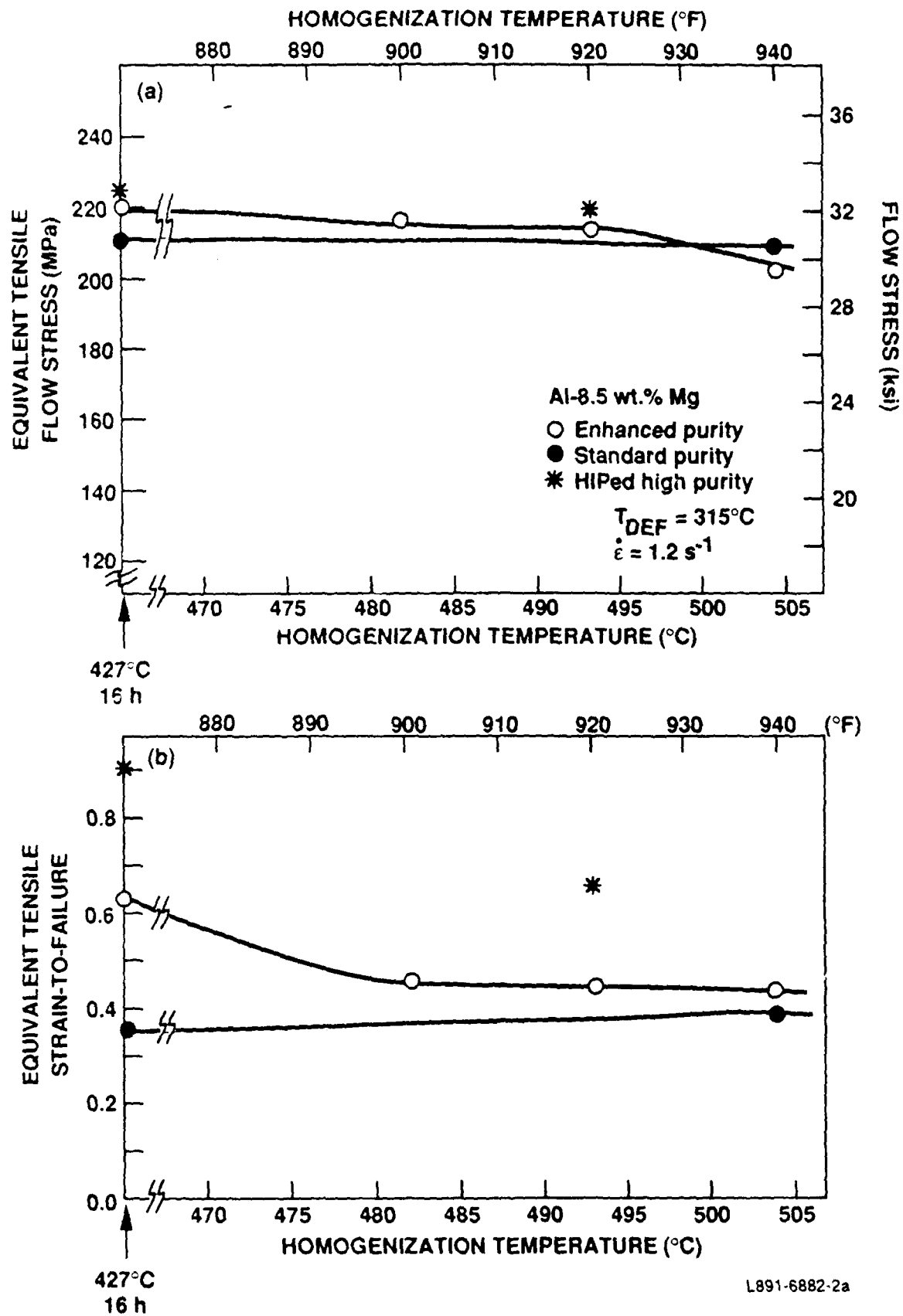


Fig. 6 Effect of homogenization temperature on a) equivalent tensile flow stress and b) equivalent tensile strain-to-failure for torsion specimens deformed at 315°C (600°F).

comparable non-HIPed specimens (Fig. 6), indicating that pore defects are partly responsible for lowering hot ductility. The flow stress and strain-to-failure data of homogenized ingot sections from which hot-torsion tests were conducted at 427°C (800°F) and an equivalent tensile strain rate of 1.2 s^{-1} are shown in Fig. 7.

The enhanced-purity alloy showed superior hot workability at all homogenization temperatures investigated. An initial homogenization treatment at 427°C (800°F) for 16 h was performed to bring the nonequilibrium eutectic β phase into solution. There was a small improvement in workability after a second-stage homogenization at or above 471°C (880°F). Strain-to-failure of the standard-purity material decreased with increasing homogenization temperature and there was a significant areal fraction of quasi-cleavage facets on the fracture surface. Little benefit was attained by increasing either the homogenization temperature beyond 471°C (880°F) or the purity level above that of the initial enhanced-purity alloy (0.049 to 0.011 wt% for Si; 0.086 to 0.044 wt% for Fe).

A similar study of the effect of homogenization temperature on strain-to-failure was also conducted at an equivalent tensile strain rate of 0.1 s^{-1} . The enhanced-purity alloy again showed significantly higher levels of ϵ_f than the standard commercial-purity alloy (see Fig. 8). The lower strain rate resulted in a substantially higher ϵ_f (about fivefold) for each purity level and a greater difference in ϵ_f between the enhanced- and commercial-purity alloys. At the lower strain rate, the hot ductility improved slightly as the homogenization temperature was increased from 471 to 482°C (880 to 900°F). Thus, the stage-2 homogenization at 482°C (900°F) was selected for all Phase II research.

B. PHASE II

In Phase I, the stage-1 homogenization at 427°C (800°F) was performed for 16 h to ensure that all β -phase (Mg_2Al_3)* had gone into solid solution before the higher temperature stage-2 treatment was performed. The resulting

*The Mg_2Al_3 phase is sometimes written as Mg_5Al_8 ; the composition range of its existence is closer to the latter stoichiometry.

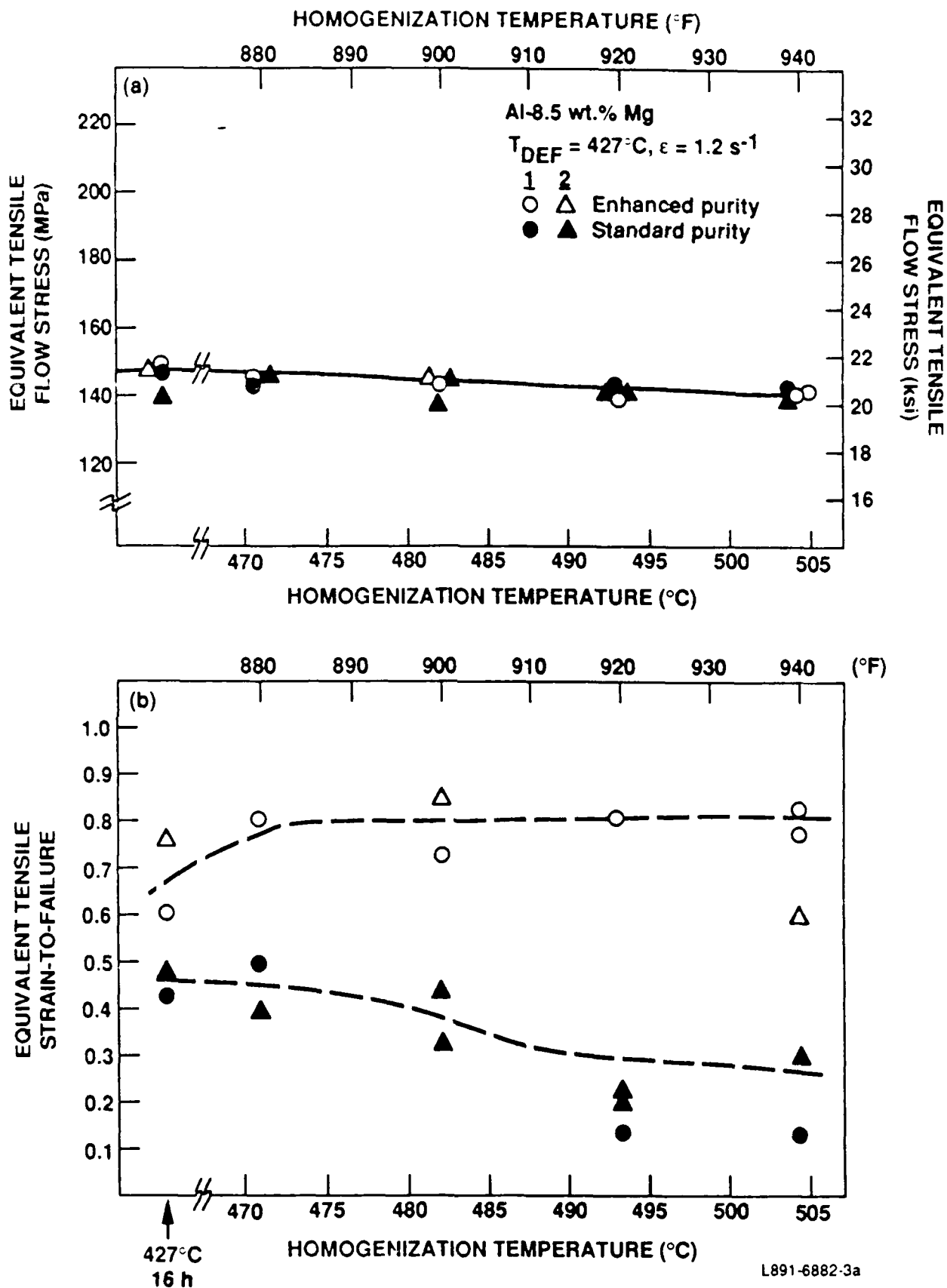


Fig. 7 (a) Flow stress and (b) strain-to-failure variation with homogenization temperature for hot torsion tests conducted at 427°C (800°F). The results for 2 ingots of each purity level are plotted.

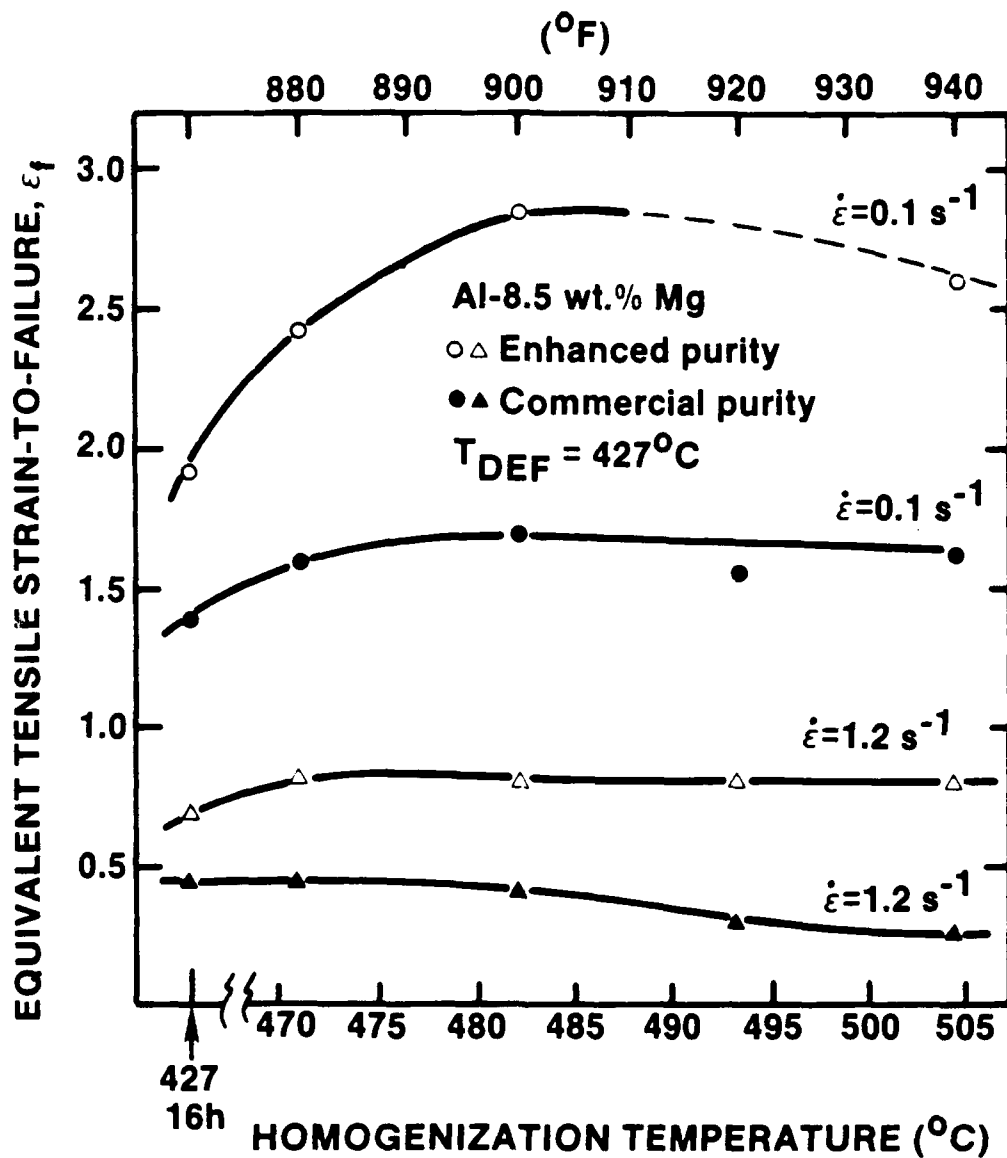


Fig. 8 Alloy purity and strain rate effects on equivalent tensile strain-to-failure for specimens homogenized at different temperatures. Homogenization temperatures are stage-2 for 8 h each and follow a stage-1 practice of 427°C for 16 h.

liquation of the Mg_2Al_3 would otherwise result in additional porosity upon further homogenization. One goal of Phase II was to optimize the homogenization times of both stages of the process. To simulate the stage-1 homogenization, sample blanks were homogenized at $427^\circ C$ ($800^\circ F$) for periods of time ranging from 0 to 16 h.

Metallographic polishing and etching of these blanks revealed that all the Mg_2Al_3 phase had gone into solid solution within 4 h. Thus, the hot-torsion specimens were subsequently given a 5 h homogenization at this temperature. Larger commercial-scale ingots may require longer homogenization times because decreased cooling rates from the melt can result in coarser β precipitates.

Stage-2 homogenization of hot torsion specimens was performed between 0 and 12 h in 2-h increments at $482^\circ C$ ($900^\circ F$). Little variation in σ_0 was apparent with increasing homogenization time for specimens deformed at $427^\circ C$ ($800^\circ F$) and 0.1 s^{-1} as shown in Fig. 9. However, the ϵ_f values increased with homogenization time up to ~6 h and leveled off thereafter, as shown in Fig. 10. Thus, optimum hot ductility at this strain rate requires a minimum of 6 h at $482^\circ C$. Metallographic examination of the homogenized structures revealed that the increased ductility with homogenization time is accompanied by the precipitation and coarsening of interdendritic $MnAl_6$ precipitates, as shown in Fig. 11.

Hot rolling typically* is performed at as high a deformation temperature as possible, without inducing hot shortness, to minimize the required roll forces. The strain rate is also kept as high as possible to maximize productivity. These two parameters generally affect the material's flow stress in opposite directions. Hot torsion data for the enhanced-purity alloy show a linear decrease in σ_0 with increasing deformation temperature at strain rates of 0.1 and 1.2 s^{-1} as seen in Fig. 12, with the higher strain rate showing higher σ_0 values.

* The commercial deformation temperature is also selected with consideration of other variables such as surface finish, migration of alloying elements to the surface, and oxidation behavior.

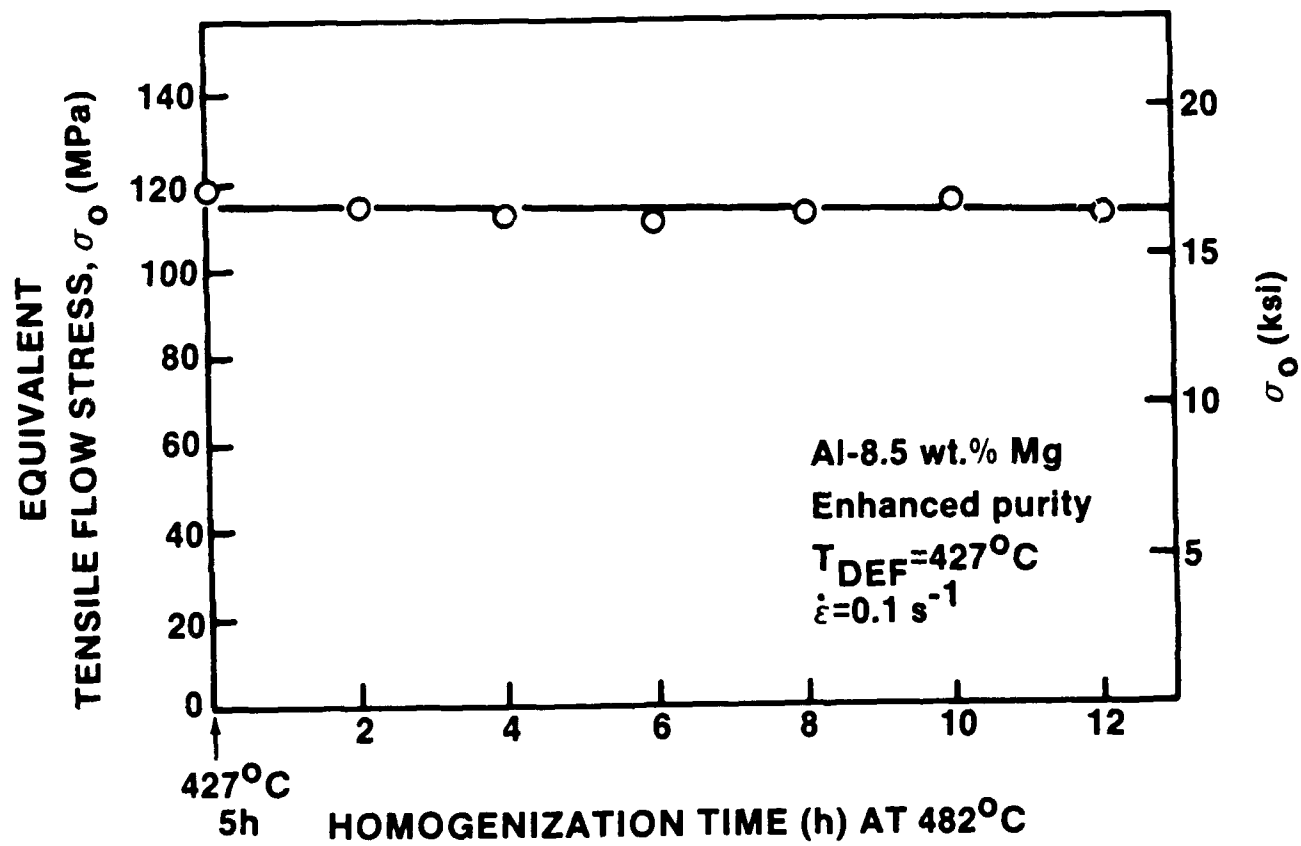


Fig. 9 Homogenization time has little influence on equivalent tensile flow stress.

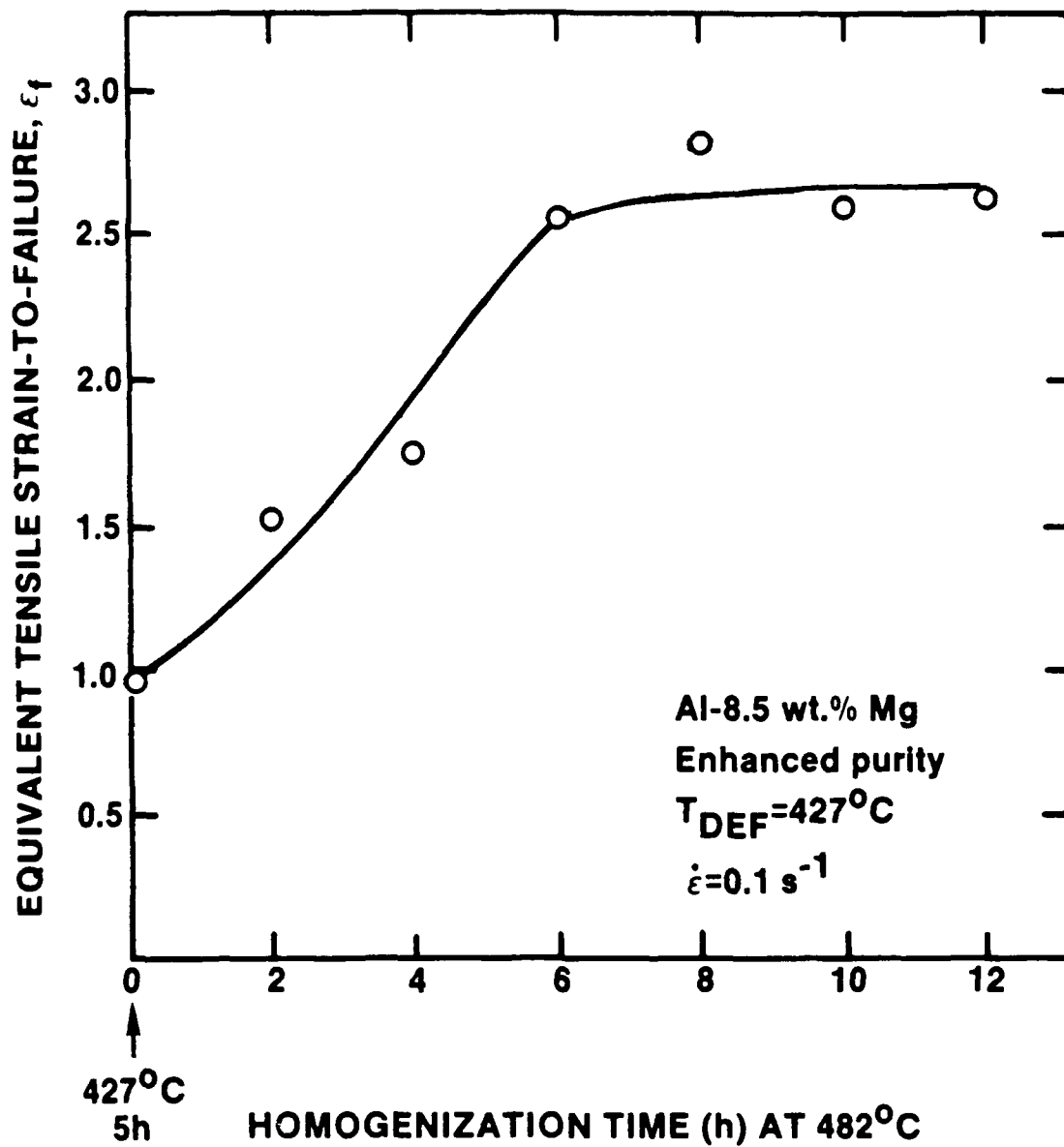


Fig. 10 Variation of strain-to-failure with homogenization time showing an increase up to ~ 6 h.

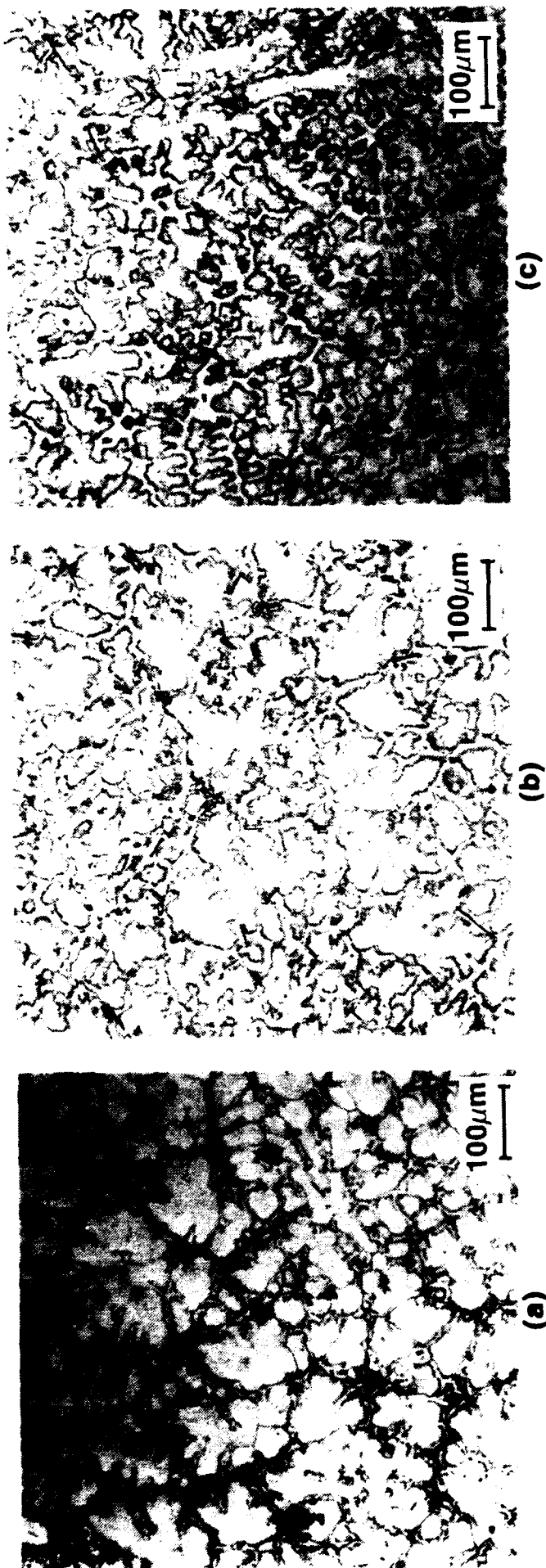


Fig. 11 Optical micrographs of enhanced-purity alloy showing interdentritic MnAl_6 precipitation and coarsening during stage-2 homogenization at 482°C (900°F) for various lengths of time: (a) 0 h, (b) 2 h, and (c) 12 h.

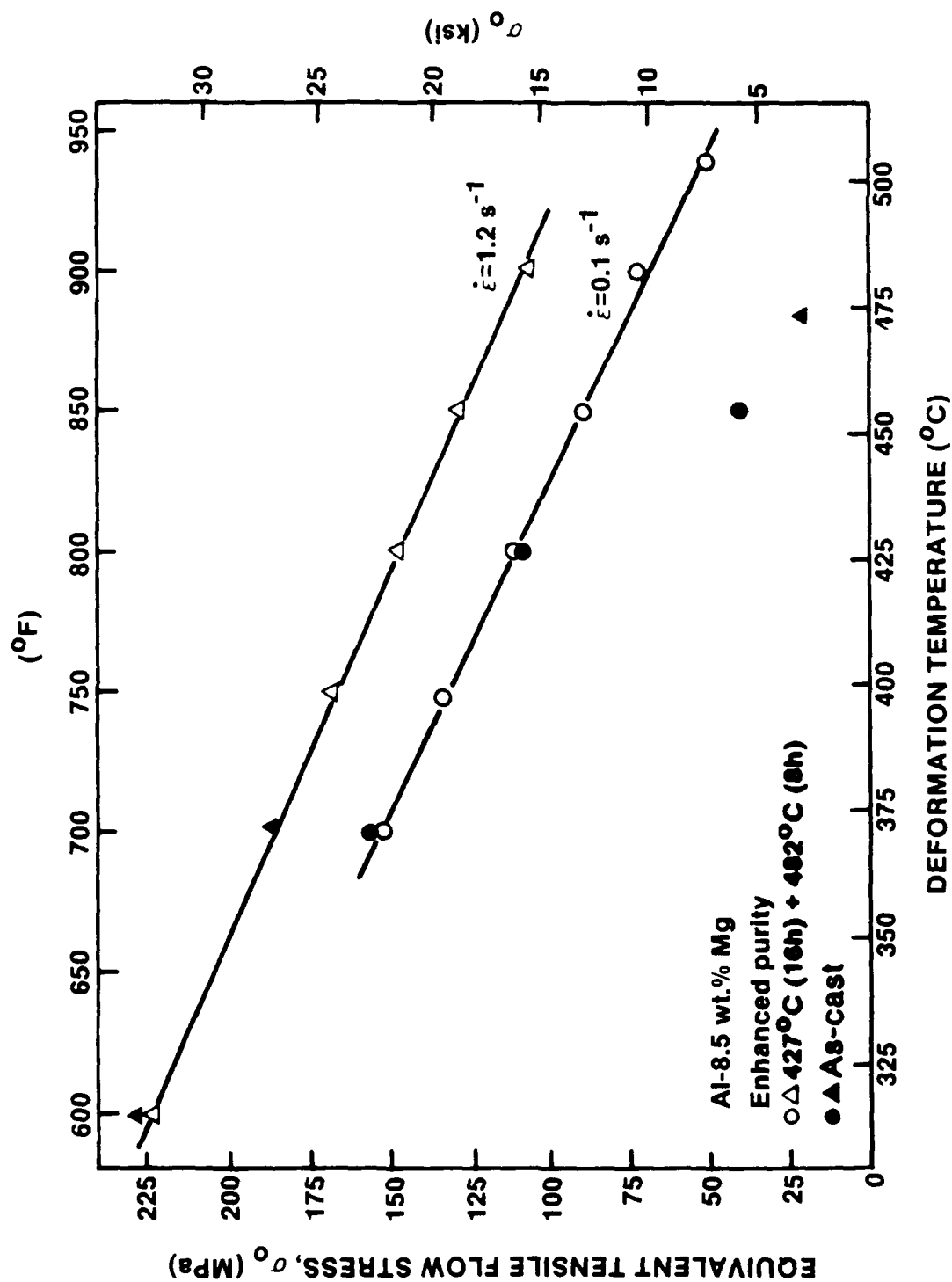


Fig. 12 Equivalent tensile flow stress decreases linearly with deformation temperature at strain rates of 0.1 s^{-1} and 1.2 s^{-1} .

Although σ_y decreases monotonically with deformation temperature, ϵ_f shows a peak between 425 and 460°C (800 and 850°F) (Fig. 13). The peak is seen at similar temperatures at both strain rates, i.e., 0.1 and 1.2 s⁻¹ but is more pronounced at 0.1 s⁻¹ where the hot ductility is higher. The rapid decrease in ϵ_f as temperature exceeds 460°C is not the result of incipient melting which, according to differential thermal analysis (DTA) and differential scanning calorimetry (DSC) of these Al-8.5% Mg alloys, only occurred above 520°C (970°F). Rather, according to fractographic examination, the decrease in ϵ_f at higher temperatures and/or higher strain rates resulted from the development of a significant areal fraction of quasi-cleavage fracture as illustrated in Fig. 14. Cleavage failure modes are rarely seen in face-centered cubic (fcc) metals such as aluminum alloys. The micromechanisms for the appearance of quasi-cleavage in Al-8.5 Mg at these temperatures is not yet clear but may be associated with stacking-fault energy effects, atomic decohesion, enhanced localized slip, or solid (or liquid)-metal-induced embrittlement from impurities such as Na, K, or Ca.

The grain size of the alloys mentioned thus far in this study ranged from 200-300 μm . With the addition of as little as 0.05 wt% Ti, the grain size decreased to 50-100 μm . Hot torsion tests of this Ti-containing alloy showed a 10% improvement in ϵ_f , e.g., at 427°C (800°F) and 0.1 s⁻¹ ϵ_f increased from 2.9 to 3.2. Interestingly, the deformed hot torsion specimens containing Ti had a considerably smoother surface topography than specimens without it, as illustrated in Fig. 15. This improvement in surface quality appears to be more than the small change in grain size would indicate and may suggest a difference in slip mechanisms. This result may also imply that a better surface quality can be obtained in the final rolled product.

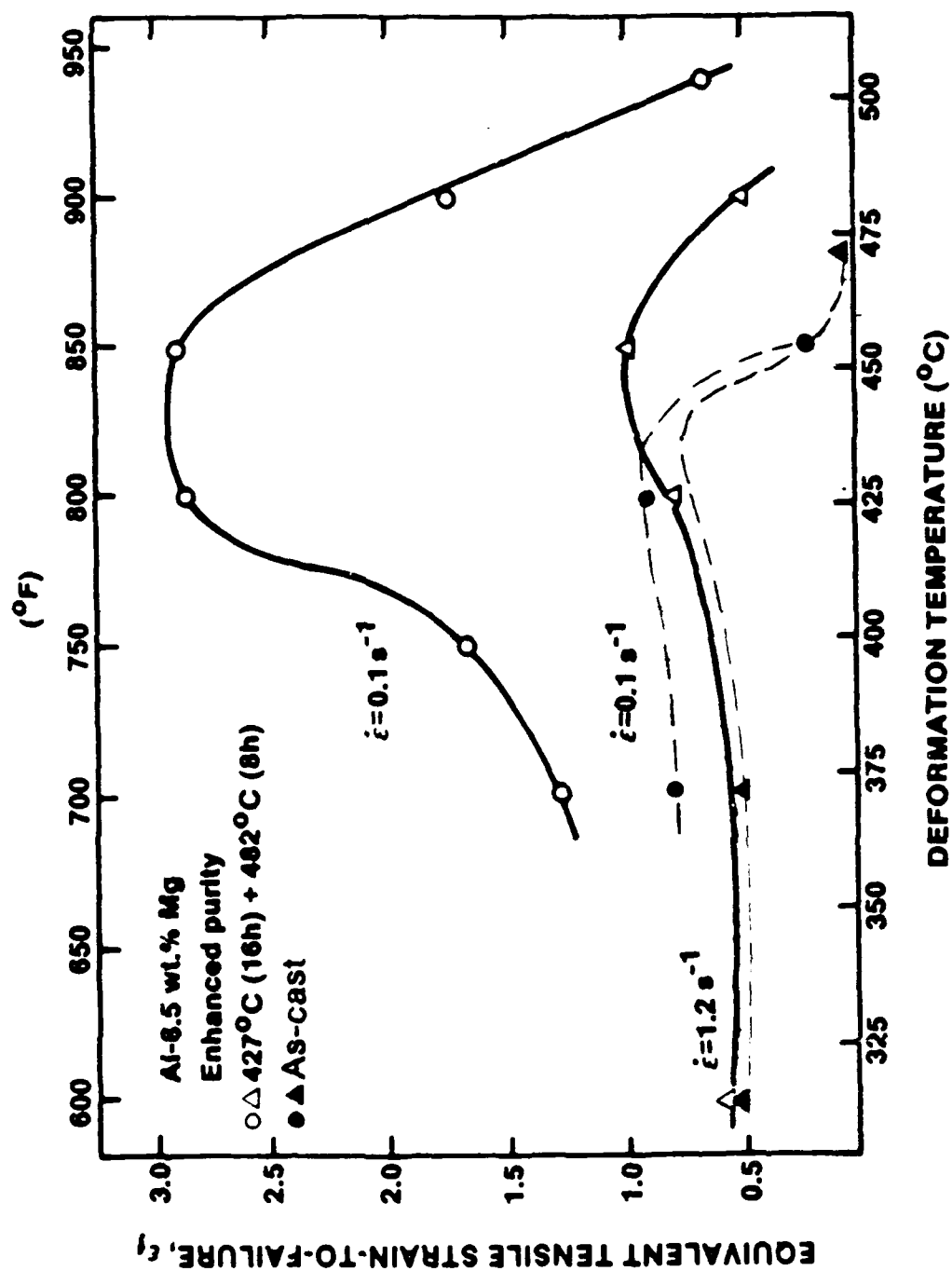


Fig. 13 Equivalent tensile strain-to-failure peaks at deformation temperatures between 425 and 460°C (800 and 850°F).

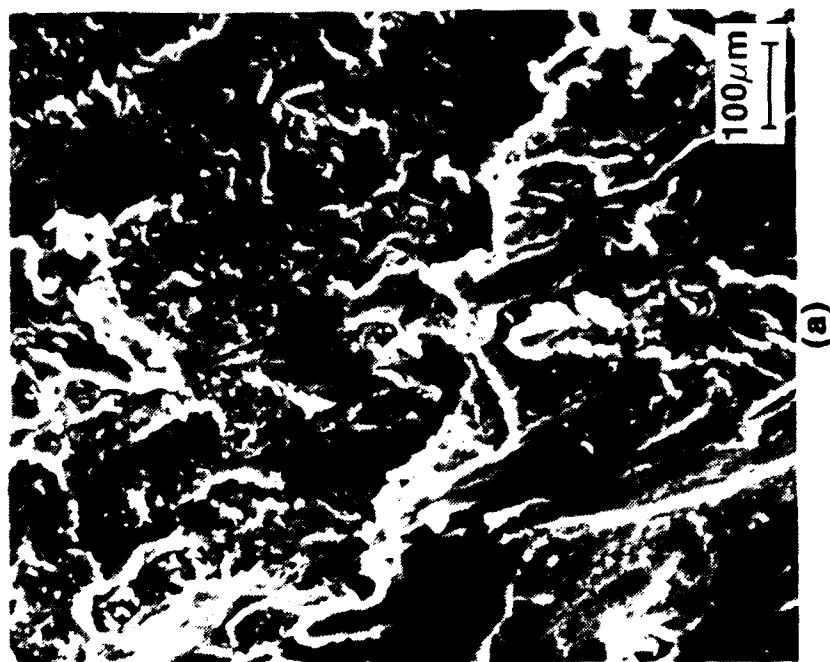


Fig. 14 Scanning electron fractographs of hot-torsion specimens deformed at 426°C showing (a) ductile shear failure at a strain rate of 0.1 s^{-1} and (b) region of quasi-cleavage at 1.2 s^{-1} . Increasing deformation temperature results in similar quasi-cleavage failure.



Fig. 15 Deformed hot torsion specimens of (a) enhanced-purity and (b) enhanced-purity with 0.05 wt% Ti, showing that the rumpling of the surface during deformation decreases with the addition of Ti to the ingot.

C. PHASE III

In this phase of the study the effects of sodium content and strain rate on hot workability of enhanced purity Al-8.5% Mg alloys were investigated. Hot-torsion tests were conducted at a deformation temperature of 427°C (800°F) and a shear strain rate of 0.1 s^{-1} on alloys containing 0 to 20 ppm sodium by weight. The results, including the mean of three tests per ingot, are summarized in Table VIII. The equivalent tensile flow stress did not significantly differ with increasing sodium levels. Surprisingly, the equivalent tensile strain-to-failure was also relatively unchanged by sodium content (0-8 ppm), except at the highest value investigated (20 ppm), where it appreciably declined (Fig. 16). Other 5xxx series alloys have been shown to be affected at much lower sodium levels. However, hot working Al-8.5% Mg alloys at much lower strain rates may minimize the relative sodium influence, as will be discussed later.

The effect of strain rate on hot workability of the alloy was examined using ingots of two different sodium levels, namely 0 and 2 ppm, the latter being a commercially feasible level for an enhanced-purity alloy. In both cases, flow stress increases linearly with increasing strain rate as shown in Table IX and in Figs. 17 and 18. Also, in both cases the equivalent tensile strain-to-failure increases with decreasing strain rate to a maximum at approximately 0.01 s^{-1} . The extremely low hot ductilities at the higher strain rates were due to the development of a cleavage-type failure mode, as was illustrated in Fig. 14. Excellent agreement between the flow stresses determined using the hot-torsion workability simulations and hot-compression testing is evident in Fig. 17.

Table VIII
Hot Torsion Data for Al-8.5% Mg Alloys with Varying Na Content
($T_{DEF} = 427^{\circ}\text{C}$, $\dot{\epsilon} = 0.1 \text{ s}^{-1}$)

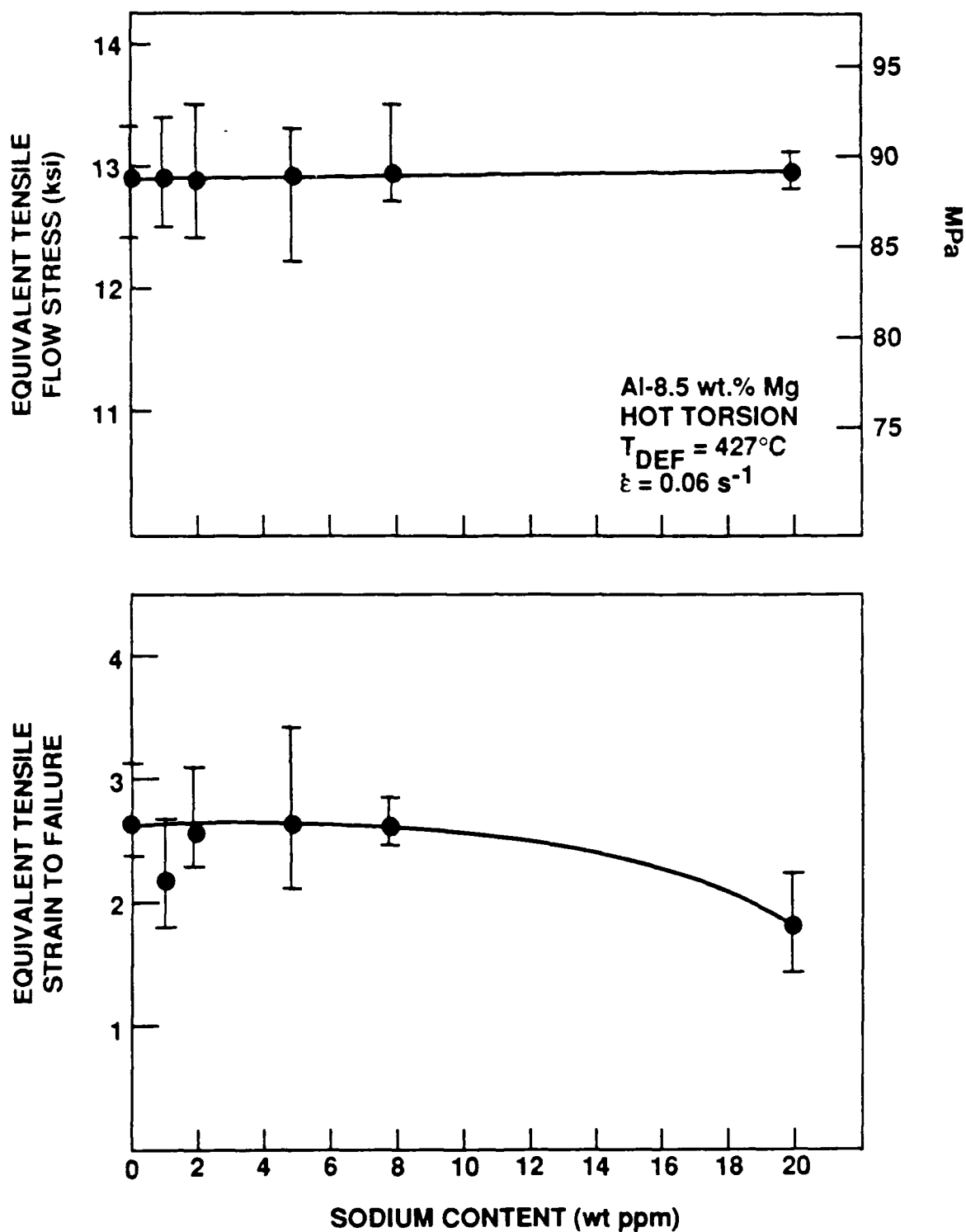
Test #	Sample #	Na (ppm)	σ_0 MPa	(ksi)	ϵ_f	ϵ_f Mean
402	1A1	0	85.5	12.4	2.37	2.64
410	1A2	0	90.3	13.1	2.39	
423	1A3	0	91.7	13.3	3.17	
403	2A1	1	86.2	12.5	2.63	2.17
411	2A2	1	88.2	12.8	1.79	
424	2A3	1	92.4	13.4	2.08	
401	3A1	2	85.5	12.4	2.27	2.57
404	3A1	2			2.73	
412	1B1	2	86.2	12.5	3.10	
405	1B1	2	93.1	13.5	2.26	
413	1B2	2	86.2	12.5	1.25 + 2.0*	
425	1B3	2	92.4	13.4	2.48	
406	2B1	5	91.7	13.3	2.56	2.76
414	2B2	5	88.2	12.8	2.32	
426	2B3	5	89.6	13.0	2.11	
407	3B1	5	90.3	13.1	3.27	
415	3B2	5	84.1	12.2	3.46	
427	3B3	5	91.7	13.3	2.83	
408	4B1	8	87.6	12.7	2.73	2.68
416	4B2	8	88.9	12.9	2.84	
428	4B3	8	93.1	13.5	2.48	
409	5B1	20	89.6	13.0	1.99	1.91
417	5B2	20	88.2	12.8	1.49	
429	5B3	20	90.3	13.1	2.25	

* Test interrupted and continued

Table IX

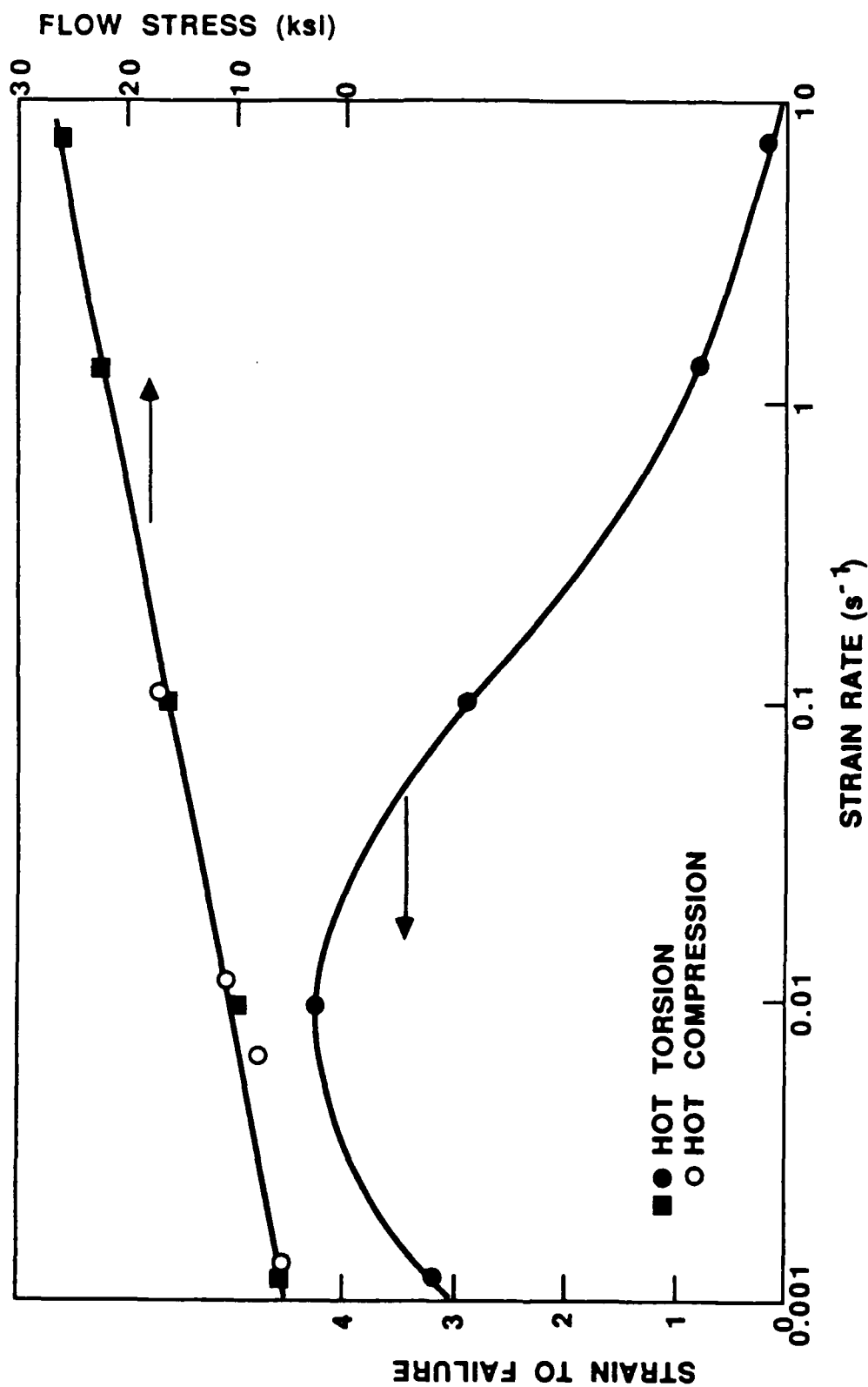
Strain-Rate Effects on Hot Torsion Study of Al-8.5% Mg
Tested at 427°C (800°F)

Test #	Sample #	Shear (s^{-1})	σ_o MPa (ksi)	ϵ_f	ϵ_f Mean
421	3A6	0.001	39.3 (5.7)	2.69	} 2.85
432	3A10	0.001	35.8 (5.2)	3.01	
418	3A3	0.01	57.9 (8.4)	3.16	} 3.51
431	3A9	0.01	60.0 (8.7)	3.86	
422	3A7	0.05	85.5 (12.4)	2.74	2.74
401	3A1	0.1	85.5 (12.4)	2.27	} 2.70
404	3A1	0.1	--	2.73	
412	3A2	0.1	86.2 (12.5)	3.10	
419	3A4	1.0	134.4 (19.4)	1.20	1.20
420	3A5	5.0	160.6 (23.3)	0.50	} 0.47
430	3A8	5.0	167.5 (24.3)	0.45	



L884-6592-3

Fig. 16 Equivalent tensile flow stress a) is unaffected by Na content and equivalent tensile strain-to-failure b) decreases above 10 ppm Na in hot torsion tests of Al-8.5Mg alloys tested at 427°C and a shear strain rate of 0.1 s^{-1} .



L882-5994-1

Fig. 17 Flow stress increases linearly with strain rate as measured using both hot torsion and hot compression testing. Strain-to-failure increases substantially with decreasing strain rate, changing from a cleavage to a ductile fracture mode.

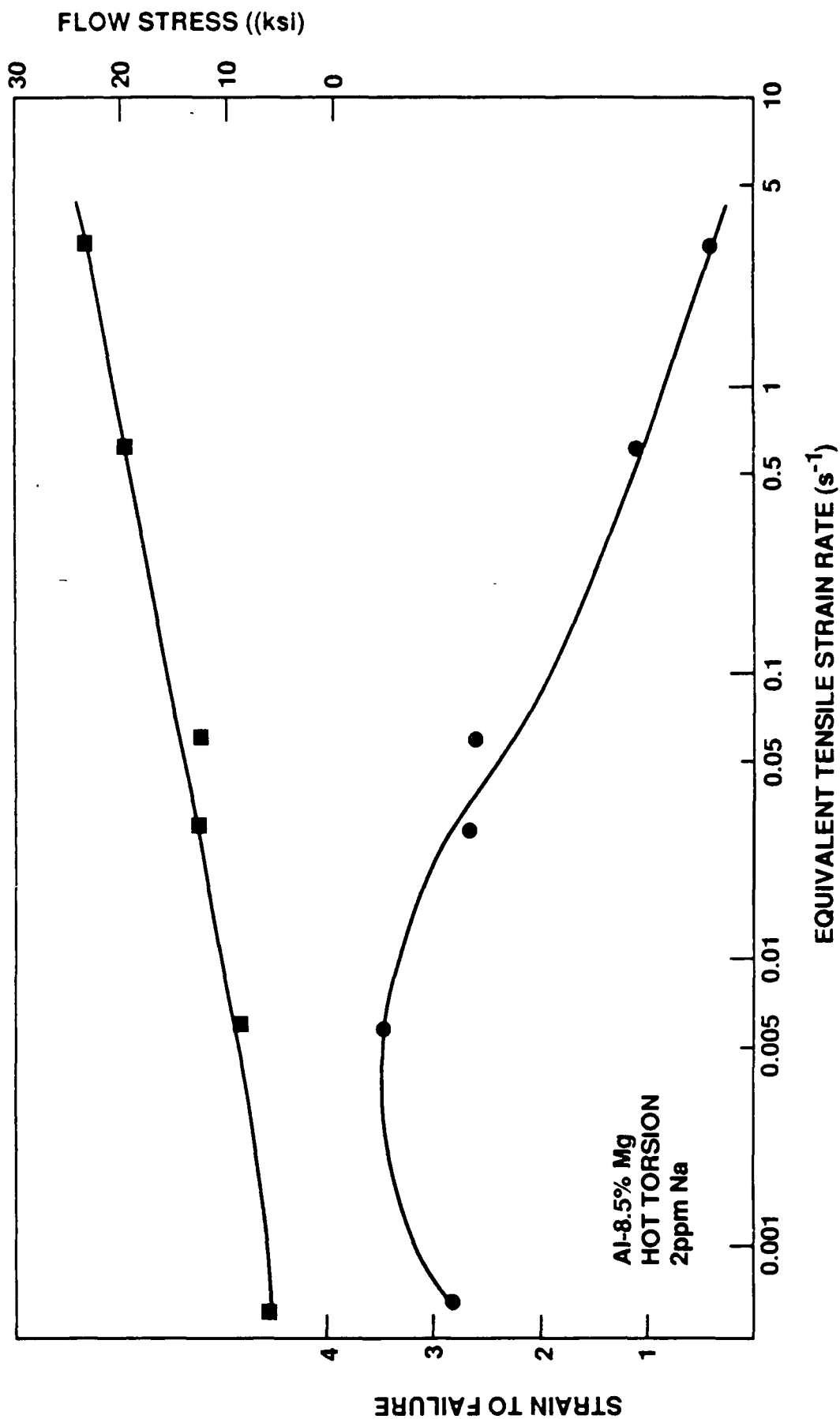


Fig. 18 Equivalent tensile flow stress and strain-to-failure of Al-8.5 wt% Mg alloy with 2 ppm sodium tested by hot torsion at 427°C (800°F) and varying strain rates.

L884-6592-2

D. ROLLING STUDY

Enhanced-purity ingots of the Al-8.5% Mg alloy were rolled using the optimized homogenization conditions, deformation temperature, and strain rates determined in the first three phases of this study. The hot-rolling schedule was summarized in Table VI. Because the rolls were not heated and the strain rate was kept low, significant heat was lost during each pass on these laboratory-scale ingots. For example, the imbedded thermocouples recorded a temperature drop of approximately 50°C (120°F) in two passes. [Note: The slabs were reheated every two passes to keep the working temperature within the optimum range]. After two or three such roll/reheat cycles, the cast structure was partially broken down four to six subsequent passes were successfully made before reheat. Thus, at this stage, a temperature drop in excess of 100°C (180°F) is tolerable. During the first pass of each ingot, large edge cracks that were several centimeters deep opened up at the drilled thermocouple hole; the remainder of the slab was almost free of edge cracks. These cracks, which nucleated at defects or stress concentrators, primarily showed the "cleavage" fracture morphology that was seen in hot-torsion specimens deformed at high strain rates. This result is significant in that it indicates the sensitivity of the alloy to cracking induced by preexisting defects during the hot rolling process. Microporosity is believed to have initiated small surface defects during the first pass and subsequently become rolled out, resulting in a checked surface appearance on some plates.

Ingots hot rolled successfully using the optimized conditions determined from the hot torsion tests. Because the as-cast structure was partially broken down after the first few passes and small internal defects such as micropores might have healed, ingot #2 was rolled at the more typical commercial rolling speed corresponding to a strain rate of 1.2 s^{-1} after 50% hot reduction. In just one pass at this speed the plate cracked severely, not only at its edges but also across its entire width and nearly through the entire thickness with a spacing of approximately 2 to 6 cm. Figure 19 is a photograph of this slab next to one of the other three that rolled



Fig. 19 Photograph of Al 8.5%Mg plate that was rolled at the optimum conditions determined from the hot torsion tests (left) and plate rolled at a strain rate of 1 s^{-1} , which cracked severely.

successfully. Scanning electron microscopy of the fracture surface from this rolled plate shown in Fig. 20 reveals a cleavage-type morphology, as in the hot-torsion samples tested under these conditions.

The hot-rolled plates at nominally 2.5 cm (1 in.) thickness were annealed at 450°C (850°F) for approximately 0.5 h prior to providing several cold rolling passes as summarized in Table VII. Although this study did not involve an optimization of cold-rolling parameters, the plates did cold roll successfully but with a few difficulties that will require further attention. Because of the extremely high work-hardening rates of these high magnesium-containing aluminum-based alloys, small reductions had to be taken on the relatively small rolling mill to keep it from stalling. On the final passes, "alligators" occasionally nucleated where the ends were folded during hot rolling, or in some cases, at the edge cracks initiated by the thermocouple hole. Such alligatoring in the cold-rolling stage could be avoided by remachining or shearing a camber or V section on the leading edge of the plate after the final hot rolling. This procedure as well as decreasing reduction per pass have been patented for commercial practice (R.N. Mitchell, British Patent #1264042, to Reynolds, 1969, W.L. Otto, et al., US Patent #4,584,862, 1986, W.L. Otto, et al., US Patent #4,593,511, 1986).

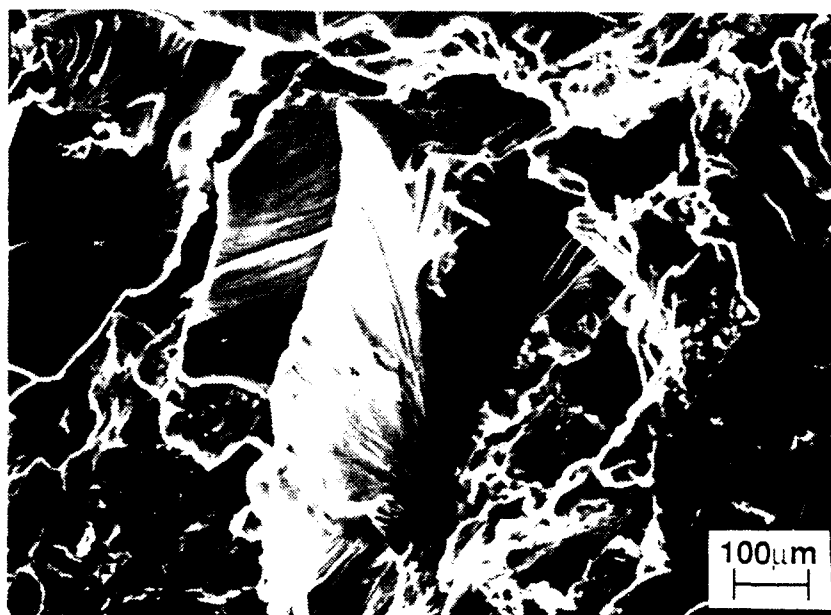


Fig. 20 Scanning electron micrograph showing a quasi-cleavage fracture mode in rolling ingot #2 which was rolled at a strain rate of $\sim 1 \text{ s}^{-1}$.

IV. DISCUSSION

Hot-torsion testing of enhanced- and standard-purity variants of Al-8.5% Mg alloys in both as-cast and homogenized conditions showed that the enhanced-purity alloy had superior hot workability at all deformation temperatures and strain rates investigated. A cost premium of 0.0201 \$/kg* for increased purity raw materials would be incurred in the commercial casting of this alloy. The enhanced purity levels of Fe and Si impurities investigated are readily producible. Typical aerospace and aircraft alloys specify tighter impurity and hydrogen tolerances. This additional initial cost for the higher purity would likely be compensated for by reduced material-scrap losses resulting from edge cracking during rolling. In addition, the higher purity variant will likely have improved fracture toughness at ambient temperature as has been demonstrated for enhanced-purity 7xxx series alloys.⁽¹²⁾

The Fe and Si impurities in the standard-purity alloy form a significant volume fraction of secondary insoluble constituent phases that can act as nucleation sites for cracks. In particular, at the higher rolling speeds used in commercial practice, quasi-cleavage cracks can form at these constituent particles and propagate unstably over considerable distances in the rolled plates.

Homogenization treatments do not affect the constituent phases containing Fe and Si but act to:

- o Bring into solid solution the nonequilibrium eutectic phase: stage-1, 427°C (800°F) for > 5 h
- o Provide a uniform distribution of unbound soluble elements e.g., Mg
- o Precipitate Mn atoms in a fine interdendritic dispersion of $MnAl_6$ from the supersaturated solid solution.

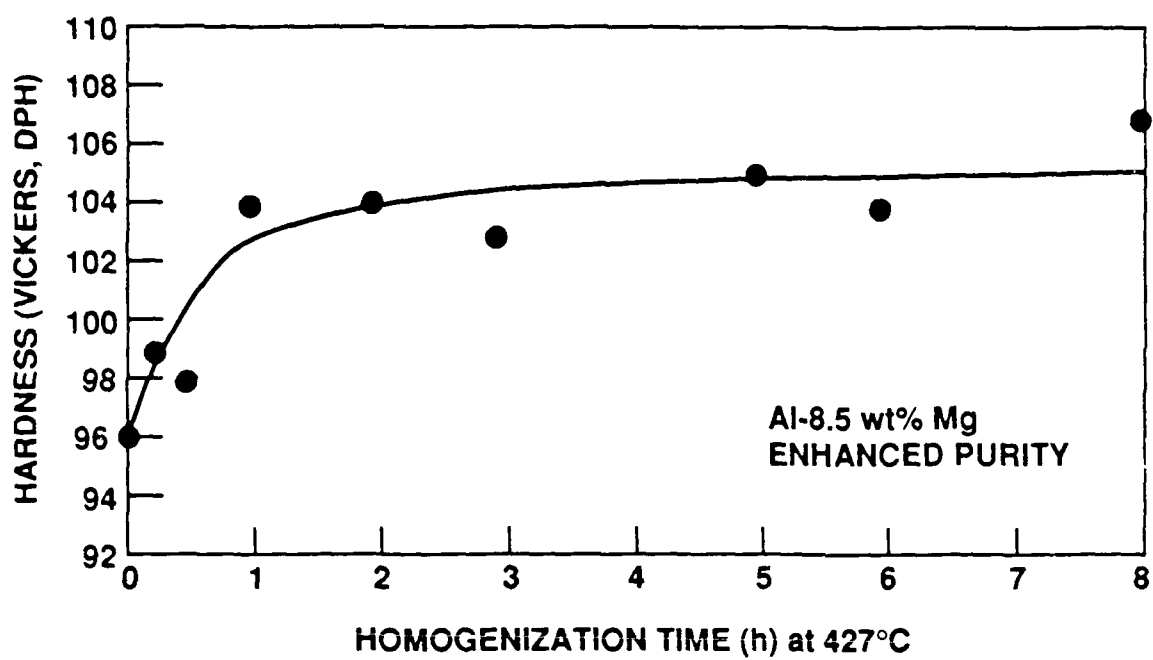
* 0.3241 \$/kg (enhanced) vs 0.3040 \$/kg (commercial)

Stage-1 homogenization acts, to some extent, on all three processes and the stage-2 homogenization treatment (471°C, 900°F for 6 h) brings the final two processes to a point where hot ductility is maximized in the minimum amount of time. Since Mg is a potent solid solution strengthening element in aluminum, hardness increases during stage-1 homogenization as seen in Fig. 21. The precipitation of $MnAl_6$ particles can also contribute to the increase in hardness with homogenization time.

Previous studies on Al-Mn alloys have shown that Mn in solid solution can have a deleterious effect on hot workability.⁽¹³⁾ This is consistent with the increase in strain to failure with homogenization time seen in Fig. 10, and the corresponding optical micrographs in Fig. 11 showing the precipitation and coarsening of the interdendritic $MnAl_6$ for the Al-8.5% Mg alloy. Lee and Wu⁽¹⁴⁾ conducted hot torsion tests on an Al-4.85% Mg alloy containing 0.7% Mn. They concluded that coarsening of a uniform distribution of the Mn-containing dispersoids is necessary for improved hot ductility and, furthermore, that Si impurities impair ductility by leading to Mn microsegregation.

Hot working of aluminum alloys, which typically have high stacking-fault energies, proceeds by way of a dynamic recovery mechanism in which dislocation interactions (e.g., glide, climb, cross-slip, and annihilation) lead to a subgrain network. Recently, dynamic recrystallization has been suggested to occur in high Mg-containing aluminum alloys such as Al-4.4%Mg-0.7%Mn-0.15%Cr alloy 5083⁽¹⁵⁾. Relatively large particles ($>0.6\mu m$), e.g., $MnAl_6$, are required to initiate dynamic recrystallization by concentrating strain in the region around the particle to serve as a driving force for the recrystallization. In addition, the lowering of the stacking fault energy by Mg contributes by promoting the formation of partial dislocations, which are less mobile than non-dissociated dislocations and consequently cannot readily climb to relax strain around the particle.

The equivalent true stress-strain curve of an alloy exhibiting dynamic recovery rises monotonically to a relatively high strain level, whereas during dynamic recrystallization, there is a gradual decline in stress following the peak flow stress. The latter is seen in the Al-8.5% Mg alloys in this



L884-6592-1

Fig. 21 Hardness increases with stage-1 homogenization time as increased Mg goes into solid solution and submicron $MnAl_6$ precipitates from supersaturated solid solution.

investigation, as reflected in the raw data (previously provided to AMTL). However, this does not unambiguously demonstrate dynamic recrystallization since both texture development and flow localization have been suggested to yield similar curves. (16)

Longitudinal sections across deformed hot torsion samples were metallographically polished, anodized, and viewed under polarized light as shown in Fig. 22 to further investigate the occurrence of dynamic recrystallization in Al-8.5% Mg alloys. Fine, recrystallized grains are evident in the highly deformed outer region of the specimen with no recrystallization near the central neutral axis. Whether this recrystallization was dynamic or static is not certain because several seconds were required to move the furnace prior to quenching, and static recrystallization might have occurred during that period.

To determine which type of recrystallization occurred, precise transmission electron microscopy would have to be performed to determine whether substructure, i.e., subgrain or extensive dislocation networks, are present in these grains. Recrystallized grains that are devoid of substructure are statically recrystallized. Those containing substructure are dynamically recrystallized.*

The activation energy, Q , of the hot-deformation processes involved during dynamic recovery of aluminum alloys is nominally the same as for lattice self-diffusion at temperatures above 60% of the absolute melting temperature (150-160 kJ/mole). For the Al-8.5% Mg alloy, Q was calculated from the creep power law:

$$\dot{\epsilon} = A\sigma_0^n \exp(-Q/RT)$$

using the data from Fig. 12. This gave $Q = 185$ kJ/mole at 400°C and

* Or "continuously recrystallized" in which case relatively low-angle boundaries slide during deformation in a manner that increases the angle of misorientation, thereby forming high angle grain boundaries in a "continuous" fashion.



Fig. 22. Optical polarized micro-photograph of a hot-drawn specimen showing spherulitic structure and necked regions. The neck diameter and neck length are indicated by the arrows.

218 kJ/mole at 450°C. Higher than expected values of Q have been reported in Al-Mg alloys because of their exceptional elevated temperature strength; that is, Mg atoms in solid solution can interact with dislocations that impede their motion⁽¹⁷⁾. Because Q changes with deformation temperature, the rate-controlling process in the deformation mechanism changes with temperature. This may result from the dominance of one of competing processes such as dynamic recovery and dynamic recrystallization in a particular temperature regime. Alternatively, different rate-controlling processes may be involved in the different temperature regimes.

It is interesting to note that the change in Q with temperature results in the linear temperature dependence of flow stress seen in Fig. 12. The corresponding strain-to-failure shown in Fig. 13 has a peak in hot ductility between about 425 and 460°C. As in other alloy systems, ductility generally increases with increasing deformation temperature since dislocation motion becomes easier and other non-conservative dislocation mechanisms such as climb become operational. The decrease in strain-to-failure above 460°C is not the result of incipient melting, as evidenced by DSC results, but rather by the transition to a quasi-cleavage failure mode. This transition may be related to the relative contributions of dynamic recovery and dynamic recrystallization as follows. During dynamic recrystallization, subgrain boundaries and dislocation arrays (to which Mg or impurity atoms such as sodium or hydrogen may have migrated) are annihilated. Crack nuclei that have formed on these substructural features could be rendered ineffective by the annihilation of the preferred fracture path and may heal or become blunted during subsequent deformation⁽¹⁸⁾. At higher temperatures, in which sufficient high localized dislocation densities have not been generated to promote dynamic recrystallization, or at higher strain rates where the kinetics of boundary migration are too slow, these crack nuclei would likely propagate catastrophically. This is consistent with the observation of quasi-cleavage at the higher deformation temperatures and strain rates.

The strain-rate sensitivity (m) was calculated from data in Figs. 17 and 18:

$$m = -\frac{d \ln \sigma}{d \ln \dot{\epsilon}} \quad \text{at constant temperature}$$

The value of m was found to vary with strain rate; at $\dot{\epsilon} = 1.2 \text{ s}^{-1}$, $m = 0.11$; at $\dot{\epsilon} = 0.1 \text{ s}^{-1}$, $m = 0.21$; and at $\dot{\epsilon} = 0.0012 \text{ s}^{-1}$, $m = 0.27$. With decreasing strain rate, the strain-rate sensitivity of the alloy is rapidly approaching the values required for superplastic behavior (>0.4). McNelley, et. al.,⁽¹⁹⁾ have, in fact, demonstrated superplastic behavior in thermomechanically processed Al-10% Mg alloys at strain rates as high as 0.002 s^{-1} at 300°C after warm rolling and annealing to obtain a finely recrystallized structure containing homogeneously distributed β and MnAl_6 precipitates. However, for superplastic deformation to take place at the warm-working temperature specified, the initial hot-working step was still required. Nevertheless, with the appropriate microstructure, and at low strain rates, Al-8.5% Mg alloys can obtain high hot-ductility.

V. SUMMARY

Hot-torsion testing was used to optimize the hot workability of an Al-8.5% Mg alloy with respect to alloy purity, homogenization practice, hot-working temperature, strain rate, and sodium content. Using the results of this hot-workability simulation, trial rolling was conducted with laboratory-scale ingots to verify these parameters and to provide AMTL with material for further study.

The main results from this investigation are:

- o The enhanced purity composition with a Ti addition (Al-8.5Mg-0.5Mn-0.1Cr-0.05Si-0.05Fe-0.01Cu-0.01Zn-0.03Ti with reduced Fe, Si, Cu, and Zn) provides improved hot ductility. This high Mg-containing alloy was shown to be extremely defect sensitive during hot working and the constituent particles formed from the impurity elements may act as preexisting defects.
- o The optimum homogenization practice consists of holding at 427°C (800°F) for ≥ 5 h to bring into solution the β phase (Mg_2Al_3) followed by ≥ 6 h at 482°C (900°F). This two-stage homogenization provides a reasonably uniform solid solution of the soluble elements such as Mg, which form a cored structure during solidification, and precipitates a fine interdendritic dispersion of $MnAl_6$, thereby removing Mn atoms from where they have been reported to impair hot ductility.
- o The deformation temperature for maximum hot ductility is between approximately 425 and 460°C (800 to 850°F). The decline in strain-to failure above 460°C is not the result of incipient melting in this alloy but the transition to a quasi-cleavage type of fracture mode.
- o The areal fraction of quasi-cleavage facets on the fracture surface increases with increasing strain rate.

- o Commercial Al-Mg alloys are typically hot worked at a mean equivalent strain rate of about 1.2 s^{-1} for maximum productivity. The Al-8.5% Mg alloy in this study must be worked at a lower strain rate of approximately 0.1 s^{-1} to obtain reasonable hot ductility and thereby minimize edge cracking.
- o For this high Mg-containing aluminum alloy, sodium from 0-8 ppm does not appear to greatly affect hot workability at the lower strain rates needed to maintain good hot ductility ($0.01\text{-}0.1 \text{ s}^{-1}$). At 20 ppm Na, a significant reduction in strain-to-failure was observed.
- o Laboratory-scale ingots were successfully rolled with minimal edge cracking using the enhanced purity material, homogenization parameters, deformation temperatures, and strain rates determined from the hot-torsion workability simulation. Thus, the hot torsion results were corroborated by actual rolling experiments. Cold rolling passes performed following hot rolling resulted in some tendency toward alligatoring.

VI. CONCLUSIONS

Hot torsion results for the Al-8.5% Mg alloys were conducted from which the following conclusions were made:

- o The enhanced-purity variant containing Al-8.5Mg-0.5Mn-0.1Cr-0.05Si-0.05Fe-0.01Cu-0.01Zn-0.03Ti demonstrated significantly higher hot ductility than standard purity with no change in flow stress.
- o The optimum homogenization practice consists of soaking at 427°C (800°F) for ~5 h plus 482° C (900° F) for ~6 h.
- o The optimum hot-working temperature is between 427° and 460°C (800-850°F).
- o Sodium levels between 0 and 8 ppm do not affect hot ductility at the optimum strain rate and deformation temperature.
- o As $\dot{\epsilon}$ decreases from 7 to 0.01 s⁻¹, ϵ_f increases from 0.2 to between 3.5 and 4.2 depending on Na level, and σ_0 decreases from 170 to 35 MPa (25 to 5 ksi).
- o In this alloy system, high strain rates or deformation temperatures lead to a quasi-cleavage failure mode. Edge cracks with this fracture morphology propagate from impurity-related defects.
- o Trial rolling of laboratory-scale ingots showed minimal edge cracking when hot rolled using the optimized parameters determined from the hot-torsion tests.

VII. RECOMMENDATIONS

The defect sensitivity of these Al-8.5%Mg alloys suggests that further work is needed to assess the use of the recommended hot working parameters on scaled-up ingot sizes cast continuously. However, hot or permanent mold castings of high strength aluminum alloys are frequently found to have higher levels of shrinkage porosity and other defects than continuously cast material. The larger ingots would retain heat over more passes than the smaller laboratory scale castings and, thus, may require fewer reheat cycles although a relatively slow strain rate will still be required, decreasing the throughput and increasing production costs. A detailed study of the cold rolling parameters is also needed to minimize the alligatoring and cold tearing which was seen in some cases in the present study. -

A detailed, fundamental investigation of the causes of the brittle quasi-cleavage failures observed during the higher strain rate or high temperature deformation is also recommended. Studies on this failure mode, rarely seen in aluminum alloys, may lead to not only interesting scientific information (such as altered dislocation and slip processes or liquid metal embrittlement components), but also further insights into altered processing parameters for increased productivity.

VII. REFERENCES

1. D.E.J. Talbot and C.E. Ransley, "The Addition of Bismuth to Aluminum-Magnesium Alloys to Prevent Embrittlement," Met. Trans. A, Vol. 8A, July 1977, pp. 1149-1154.
2. C.E. Ransley and D.E.J. Talbot, "The Embrittlement of Aluminum-Magnesium Alloys by Sodium," J. Inst. Met., Vol. 88, 1959-1960, pp. 150-158.
3. P.F. Thomson and N.M. Burman, "Edge Cracking in Hot-Rolled Al-Mg Alloys," Mater. Sci. Eng., Vol. 45, 1980, pp. 95-107.
4. R.L. Cheek, "Aluminum Industry Problems with Magnesium Usage," in Proc. Int. Magnesium Assoc., 35th Annual Meeting, 25-26 June 1978, Spokane, WA, pp. 6-9.
5. C.M. Sellers and W.J. McG. Tegart, "Hot Workability," Intl. Met. Rev., Vol. 17, 1972, pp. 1-24.
6. P. Moore, "Methods for Studying Hot Workability: A Critical Assessment," in Deformation Under Hot Working Conditions, ISI Special Report 108, 1968, pp. 103-106.
7. I. Weiss, J.J. Jonas, and G.E. Ruddle, "Hot Strength and Structure in Plain C and Micro-alloyed Steels During the Simulation of Plate Rolling by Torsion Testing," in Proc. ASM Symp. Process Modelling Tools, ASM Publication, Metals Park, OH (1980).
8. J.R. Pickens, W. Precht, and J.J. Mills, "Hot Rolling Simulation of Electromagnetically Cast and Direct-Chill Cast 5182 Aluminum Alloy by Hot Torsion Testing," in Innovations in Materials Processing, Proc. 30th Sagamore Army Mat'l. Res. Conf., August 1983, G. Bruggeman and V. Weiss, eds., pp. 101-115.

9. W. Precht and J.R. Pickens, "A Study of the Hot Working Behavior of Al-Mg Alloy 5052 by Hot Torsion Testing," Met. Trans. A, Vol. 18A, Sept. 1987, pp. 1603-1611.
10. J.R. Pickens, W. Precht, and J. Mills, to be published.
11. D.S. Field and W.A. Backofen, "Determination of Strain Hardening Characteristics by Torsion Testing," in Proc. ASTM, 1957, Vol. 57, pp. 1259-1272.
12. E. Evangelista, E. DiRusso, H.J. McQueen and P. Mengucci, "Mechanical Improvements in 7xxx Alloys by Different Alloying Balance," in Homogenization and Annealing Aluminum and Copper Alloys, Conference Proceedings from ASM, TMS-AIME, Oct. 1987.
13. L.F. Mondolfo, Manganese in Aluminum Alloys, The Manganese Center, p. 96.
14. S.L. Lee and S.T. Wu, "Influence of Soaking Treatments on Hot Ductility of Al-4.85 Pct Mg Alloys Containing Mn," Met. Trans. A, Vol. 17A, 1986, pp. 833-841.
15. H.J. McQueen, E. Evangelista, J. Bowles and G. Crawford, Met. Sci. Vol. 18, 1984, pp. 395-402.
16. H.J. McQueen and D.L. Bourell, "Hot Workability of Metals and Alloys," J. Metals, 1987, pp. 28-36.
17. J.R. Cotner and W.J. McG. Tegart, "High-Temperature Deformation of Aluminum-Magnesium Alloys at High Strain Rates," J. Inst. Met., Vol. 97, 1969, p. 73.
18. A.T. Cole and G.J. Richardson, Hot Working and Forming Processes, The Metals Society, London, 1979, p. 128.

19. T.R. McNelley, E.W. Lee, and M.E. Mills, "Superplasticity in a Thermomechanically Processed High-Mg, Al-Mg Alloy," Met. Trans. A, Vol. 17A, 1986, pp. 1035-1050.

VIII. ACKNOWLEDGEMENT

The authors are grateful to Dr. Judy Kohatsu, under whose auspices this program strated, for her enthusiastic technical contributions and support. We also appreciate the efforts of B. Ward and D. Wiggins at Reynolds Metals Company for their rolling expertise and suggestions on sodium measurement. Finally, we appreciate the continued support of E. Chin, Dr. P.L. Fopiano, M.R. Cappucci, and Dr. M.G.H. Wells throughout the life of this program, which was supported by the Army Materials Technology Laboratory under Contract No. DAAG46-85-C-0034.